

Copyright Warning & Restrictions

The copyright law of the United States (Title 17, United States Code) governs the making of photocopies or other reproductions of copyrighted material.

Under certain conditions specified in the law, libraries and archives are authorized to furnish a photocopy or other reproduction. One of these specified conditions is that the photocopy or reproduction is not to be “used for any purpose other than private study, scholarship, or research.” If a user makes a request for, or later uses, a photocopy or reproduction for purposes in excess of “fair use” that user may be liable for copyright infringement,

This institution reserves the right to refuse to accept a copying order if, in its judgment, fulfillment of the order would involve violation of copyright law.

Please Note: The author retains the copyright while the New Jersey Institute of Technology reserves the right to distribute this thesis or dissertation

Printing note: If you do not wish to print this page, then select “Pages from: first page # to: last page #” on the print dialog screen

The Van Houten library has removed some of the personal information and all signatures from the approval page and biographical sketches of theses and dissertations in order to protect the identity of NJIT graduates and faculty.

ABSTRACT

RHEOLOGICAL CHARACTERIZATION OF UNMODIFIED AND CHEMICALLY MODIFIED POLY(ETHYLENE TEREPHTHALATE) RESINS

by
Jorge Quintans

Intrinsic viscosity (IV) has often been misused for estimating both melt viscosity and elasticity of poly(ethylene terephthalate) (PET). A rheological study was conducted to determine the variations between a virgin unmodified PET and a recycled and chemically modified PET, both having a reported nominal IV of 0.95.

The modified material had a larger melt viscosity (capillary and dynamic) than the virgin material (by an average of 61%). The extrudate swell, a better indicator of melt elasticity, of the modified was more than 110% greater than that of the unmodified material. Activation energies for melt viscosity and extrudate swell were found to be approximately 20 kJ/mol and 3 kJ/mol respectively, for the unmodified material at high shear rates. The melt viscosity for both materials was found to be best fitted by the Cross Model using a least-squares fit.

**RHEOLOGICAL CHARACTERIZATION OF UNMODIFIED AND
CHEMICALLY MODIFIED POLY(ETHYLENE TEREPHTHALATE) RESINS**

**by
Jorge Quintans**

**A Thesis
Submitted to the Faculty of
New Jersey Institute of Technology
in Partial Fulfillment of the Requirements for the Degree
of Master of Science in Chemical Engineering**

**Department of Chemical Engineering,
Chemistry, and Environmental Science**

May 1998

APPROVAL PAGE

RHEOLOGICAL CHARACTERIZATION OF UNMODIFIED AND
CHEMICALLY MODIFIED POLY(ETHYLENE TEREPHTHALATE) RESINS

Jorge Quintans

Dr. Marino Xanthos, Thesis Advisor Date
Associate Professor of Chemical Engineering, Chemistry, and
Environmental Science, NJIT

Dr. Ulku Yilmazer, Committee Member Date
Visiting Professor of Chemical Engineering, Chemistry, and Environmental Science, NJIT

Dr. Piero M. Armenante, Committee Member Date
Professor of Chemical Engineering, Chemistry, and Environmental Science, NJIT

BIOGRAPHICAL SKETCH

Author: Jorge Quintans

Degree: Master of Science

Date: May 1998

Undergraduate and Graduate Education:

- Master of Science in Chemical Engineering,
New Jersey Institute of Technology, Newark, NJ, 1998
- Bachelor of Science in Chemical Engineering,
Rensselaer Polytechnic Institute, Troy, NY, 1996

Major: Chemical Engineering

Presentations and Publications:

Quintans, J., "Rheological Characterization of Virgin and Modified Recycled PET", Proceedings of the Eighth Annual Uni-tech Student Conference on Science and Technology, Newark, NJ (April 1998).

Quintans, J., Marino Xanthos, and Ulku Yilmazer, " Rheological Characterization of Virgin and Modified Recycled PET", To Appear in Proceedings of the PPS North American Meeting, Toronto, Ontario, Canada (August 1998).

This thesis is dedicated to my parents,
Manuel Quintans Rebodero and Paulina Caamaño Rey

ACKNOWLEDGMENT

The author wishes to express his gratitude to his advisor, Professor Marino Xanthos, for his guidance, friendship, and moral support throughout this research. This project would not have been possible without the help of Professor Ulku Yilmazer, Dr. Subir K. Dey, and Mr. Qiang Zhang and their words of wisdom and direction.

Special thanks to Dr. Armenante, and Dr. Yilmazer for serving as committee members.

The author is grateful to the Center for Processing of Plastics Packaging (CPPP), the Chemical Engineering Department of NJIT, and Multi-Lifecycle Engineering Research Center for funding this research.

Members of the New Jersey Bell Plastics Laboratory: Dale J. Conti, Yufu Li, and Prakash Natarajan provided timely and expert assistance in time of need. Dr. Victor Tan of the Polymer Processing Institute (PPI) in Hoboken, NJ also contributed to this project.

And finally, a thank you to Robert C. Liander Jr., Andrew A. Hanniffy, A. Scott Ferguson, and Dennis Gibney for their contributions outside the research lab. "Because it all falls within the loop".

TABLE OF CONTENTS

Chapter	Page
1 INTRODUCTION.....	1
1.1 Prelude	1
1.2 Objective	3
2 EXPERIMENTAL	5
2.1 Apparatus for Capillary Rheometry	5
2.2 Procedure for Capillary Rheometry	5
2.3 Dynamic Mechanical Data.....	7
2.4 Modeling.....	8
3 THEORY	9
3.1 Capillary Data	9
3.2 Dynamic Mechanical Data.....	10
3.3 Data Analysis	12
3.4 Modeling.....	14
4 RESULTS	17
4.1 Viscosity	17
4.2 Extrudate Swell	20
4.3 Activation Energy.....	22
4.4 Complex Viscosity Determination	27
4.5 Modeling.....	30

TABLE OF CONTENTS
(continued)

Chapter	Page
5 CONCLUSIONS.....	33
APPENDIX A EXPERIMENTAL CAPILLARY DATA FOR SHELL 9506 PET.....	35
APPENDIX B EXPERIMENTAL CAPILLARY DATA FOR REX15/F PET.....	47
APPENDIX C CORRECTED DATA AND CALCULATION RESULTS.....	55
APPENDIX D MODELING RESULTS.....	61
APPENDIX E MATLAB MODELING FUNCTIONS AND COMPUTER CODE.....	64
WORKS CITED	69

LIST OF TABLES

Table	Page
C - 1 Rabinowitsch Correction (R_C) for Shell 9506 at 290 °C	55
C - 2 Rabinowitsch Correction (R_C) for Shell 9506 at 280 °C	55
C - 3 Rabinowitsch Correction (R_C) for Shell 9506 at 270 °C	55
C - 4 R_C Curve Equations for Shell.....	55
C - 5 Corrected Data for Shell PET 9506	56
C - 6 Corrected Data for Sinco B PET.....	56
C - 7 Rabinowitsch Correction (R_C) for Sinco B at 290 °C.....	57
C - 8 Rabinowitsch Correction (R_C) for Sinco B at 280 °C.....	57
C - 9 R_C Curve Equations for Sinco B	57
C - 10 Activation Energy Dependence on Shear Rate for Shell 9506.....	59
C - 11 Complex Viscosity Data for Shell 9506	59
C - 12 Complex Viscosity Data for Sinco B	60
C - 13 R^2 Values for Shell 9506 Viscosity Fitting.....	60
C - 14 R^2 Values for Sinco B Viscosity Fitting	60

LIST OF FIGURES

Figure	Page
2.1 Rheometer Schematic.....	6
2.2 Mechanical Spectrometer Schematic	8
3.1 General Extrudate Swell Curve.....	13
4.1 Viscosity vs. Shear Rate for Shell 9506 at 290 °C.....	18
4.2 Viscosity vs. Shear Rate at 290 °C	19
4.3 Extrudate Swell Ratio vs. Shear Rate at 290 °C	22
4.4 Determination of E_v of Melt Viscosity for Shell 9506.....	23
4.5 Activation Energy of Melt Viscosity vs. Shear Rate for Shell 9506	23
4.6 Determination of E_e of Melt Elasticity for Shell 9506.....	24
4.7 Activation Energy of Melt Elasticity vs. Shear Rate for Shell 9506	25
4.8 Comparison of E_v of Melt Viscosity for Shell 9506 and Sinco B.....	26
4.9 Comparison of E_e of Melt Elasticity for Shell 9506 and Sinco B.....	26
4.10 Complete Viscosity Curve for Shell 9506	27
4.11 Complete Viscosity Curve for Sinco B	27
4.12 Viscosity vs. Shear Rate at 290 °C (Complete Curve).....	28
4.13 G' and G'' for Shell 9506 and Sinco B at 290 °C	30
4.14 Cross Model of Shell 9506 at 280 °C	31
C - 1 Rabinowitsch Correction Curves for Shell 9506 and Sinco B.....	57
C - 2 Corrected Shear Rate vs. Shear Stress for Shell 9506 PET.....	58
C - 3 Corrected Shear Rate vs. Shear Stress for Sinco B PET	58

LIST OF FIGURES
(continued)

Figure	Page
C - 4 Swell ratio and Swell % vs. Shear Rate for Shell 9506	58
C - 5 Swell Ratio and Swell % vs. Shear Rate for Sinco B	59
D - 1 Determination of n for Shell 9506 at 270 °C.....	61
D - 2 Determination of n for Shell 9506 at 280 °C.....	61
D - 3 Determination of n for Shell 9506 at 290 °C.....	61
D - 4 Determination of n for Sinco B	61
D - 5 Modeling of Shell 9506 at 290 °C.....	62
D - 6 Modeling of Sinco B at 290 °C.....	63

LIST OF SYMBOLS

$\dot{\gamma}_a$	- Apparent Shear Rate	(s ⁻¹)
$\dot{\gamma}_w$	- True (Corrected) Shear Rate	(s ⁻¹)
γ'	- In-Phase Shear Strain	
γ''	- Out-of-phase Shear Strain	
σ or σ_w	- Shear Stress	(kdynes/cm ²)
σ'	- In-phase Shear Stress	(kdynes/cm ²)
σ''	- Out-of-phase Shear Stress	(kdynes/cm ²)
M	- Torque	(g•cm)
θ	- Shearing Angle	(radians)
** All values above are measured at the wall (capillary) or edge (dynamic) **		
η	- True Viscosity	(Pa•s)
η_a	- Apparent (Uncorrected) Viscosity	(Pa•s)
η'	- In-phase Viscosity	(Pa•s)
η''	- Out-of-phase Viscosity	(Pa•s)
η^*	- Complex or Dynamic Viscosity	(Pa•s)
η_0	- Zero Shear Rate Viscosity	(Pa•s)
G'	- Storage (In-phase) Modulus	(Pa)
G''	- Loss (Out-of-phase) Modulus	(Pa)
G*	- Complex or Dynamic Modulus	(Pa)
K	- Complex Correction Factor and Power Law Constant	
ω	- Frequency	(rad/s)
n	- Power Law Index	
E _‡	- Constant Shear Rate Activation Energy	(kJ/mol)
T	- Temperature	(°C or K)
A	- Activation Energy Constant	
Q	- Volumetric Flowrate	(mm ³ /s)
R	- Die Radius	(mm)
R _C	- Rabinowitsch Correction Value	
R ²	- Coefficient of Determination	
R _g	- Gas Constant	(8.314 J/mol K)
τ	- Characteristic Time Constant	(s)
a	- Vinogradov Constant	

CHAPTER 1

INTRODUCTION

1.1 Prelude

Recycling has grown in popularity in recent times not only because of public concern but also due to political pressure. Plastics recycling has also grown and, as a result, the need to use recycled plastics for alternative applications. Following their market growth, the recycling of polyethylene terephthalate (PET) containers has also increased. Recent research and development projects have begun to explore the area of new applications of recycled PET.

Extrusion foaming is a new technology that is now starting to be applied to recycled polymers. It produces material with lower density leading to a decrease in material use while providing a useful structure. Most foaming is done with chemical blowing agents (CBA), but polymers are also foamed using VOC's, HCFC's, and gases such as CO₂, N₂, Ar, and air. In attempting to foam, the plastic used must be able to hold bubbles within the melt until the material cools and the foam structure is "frozen". Therefore, materials that have high melt strength or melt elasticity are required for good foaming, otherwise most of the gas will not be trapped in the melt and few bubbles will be formed. When dealing with polymers, the melt viscosity is often measured or quantified as an intrinsic viscosity (IV), which is a solution viscosity that is independent of the influence of entanglements [1]. When a polymer is processed, the material may be degraded and its melt viscosity, which is directly related to IV, may be reduced leading

to the problem of recycled material being "inferior" to unused or virgin material. There have been many publications involving chemical modification with multifunctional reactants of recycled material in order to increase IV and its melt strength, such as recent work by Al Ghatta, Cobror, and Severini on PET [2]. The process used by Al Ghatta is a low temperature (to minimize degradation) solid-state polyaddition that increases IV from an average of 0.6 to 0.8 or higher over 24 hours. Along with publications, there are also numerous patents which involve claims of increasing IV to specific values [3, 4, 5]. Unfortunately, since IV does not include the influence of entanglements, it is not a good measure or comparable quantity when dealing with foaming. The more entanglements present, the higher the melt strength and thus the more bubbles or gas the material can hold.

In a recent study by Xanthos et al. [6], chemically modified and unmodified PET were compared in extrusion foaming using a rod die. Melt elasticity has been shown to be a parameter of practical importance which could not only be related to extrudate swell, but also normal stress, recoverable strain, extensional viscosity, and storage modulus [7]. Low melt viscosity and low melt elasticity were found to lead to poor cell expansion, high density, and overall poor foaming. When CO₂ was used in foaming, recycled unmodified PET could not be foamed, virgin PET foamed poorly with large bubbles and high density (low density being desired), while the modified recycled PET foamed very well with low density (high swell) and fine and uniform cells. The unfoamable recycled PET was reported to have a nominal IV of 0.7, the virgin PET was 0.95, and the modified recycled PET was 0.95.

1.2 Objective

This study was conducted to perform a rheological characterization on a virgin PET and a recycled PET that has been chemically modified such that it has the same IV as the virgin. Even though the two materials have the same nominal IV, they can differ greatly in melt viscosity and melt strength. A more appropriate measure of melt strength is the extrudate swell or "die swell" of a material as it exits a die. This phenomenon is the result of the tendency of the polymer molecules to return to their original entangled position after being stretched through flowing [8]. Extrudate swell would have to be measured at steady flow, isothermal condition without sagging caused by gravity acting on the material already out of the die to provide accurate and reproducible results.

The extrudate swell is dependent on several factors, but under the same conditions materials with similar IVs can have different degrees of swelling (measured as swell ratio: the extrudate diameter divided by the die diameter). By suitable characterization techniques, one can determine the factors affecting extrudate swell (melt strength) and perhaps the quantities one can use to classify or compare these properties to those of other materials. As foaming increases in popularity and industry use, these quantities will gain importance in order to classify potential materials for products from recycled waste streams. The measurement of these quantities could also lead to further study and commercialization of instruments such as the die swell tester from C.W. Brabender Instruments Inc., based on work by I. Pliskin [9] and P. van Buskirk [10]. Besides Brabender Instruments, others have proposed a new quantity to measure melt elasticity such as Maxwell who proposed a Melt Elasticity Index (MEI), similar to the

Melt Flow Index (MFI) or just Melt Index (MI) [11]. He did not use extrudate swell as measure for melt elasticity, but instead used the amount of recoverable strain that takes place within the first 20 seconds of recovery. The importance of measuring melt elasticity was discussed, especially within quality control areas. The quantities of IV and MI, that are currently used very frequently, do not represent melt strength sufficiently.

CHAPTER 2

EXPERIMENTAL

2.1 Apparatus for Capillary Rheometry

The viscosity and extrudate swell data were determined using a Kayeness capillary rheometer with a die radius of 0.523 mm and 15 length/diameter (L/D), along with barrel diameter of 4.75 mm. Measurements were taken from 270 °C to 290 °C (± 0.3 °C) within the shear rate of 134 s^{-1} to 13340 s^{-1} , which include industrial processing ranges. The unmodified PET was Shell 9506 with a nominal I.V. of 0.95 and the modified recycled PET was PET rex15/F from Sinco Ricerche S.p.A. (referred to as Sinco B) with a nominal I.V. of 0.95 (0.7 I.V. before the chain extending modification using solid state method). The extrudate swell measurements were taken using a CCD camera / recorder / TV setup, shown in Fig. 2.1, at a distance of 9 mm from the die exit. The die swell was recorded and then analyzed using an on screen scale provided by a scaled recticle within the microscope (showing 15 mm for 0.2 mm actual length).

2.2 Procedure for Capillary Rheometry

The material (in the form of pellets) had to first be dried, usually over night or for one day at 200 °F to 250 °F, because of the degradation of PET during processing in the presence of water [12]. The rheometer used needed to be programmed with the die dimensions and the process conditions desired, including plunger rate (which determines

the shear rate). After the barrel reached the desired temperature, the dried material was packed into the barrel and the plunger was lowered immediately to provide the least amount of contact with the atmosphere as possible.

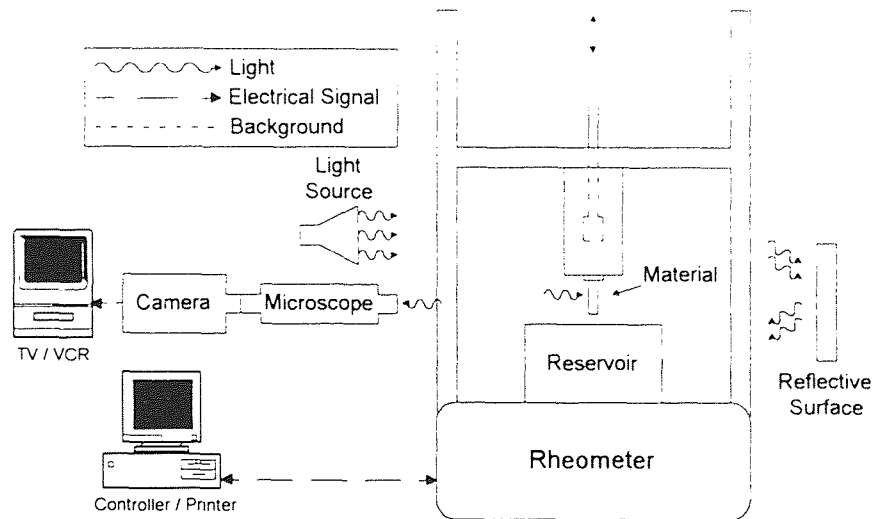


Figure 2.1 Rheometer Schematic

The material was then allowed to melt and reach a constant temperature (usually for a few minutes). The plunger was then lowered to the starting height and the rheometer program started. The program contains a melt time countdown (60 s) after which the plunger is lowered at the programmed speed, forcing the material through the barrel. Once the exiting material became uniform, the video system was started to record the extrudate swell. The material then deposited into the reservoir (a large water bath in our case) so that it no longer affected the material exiting the die or the swelling. Many studies have measured the swell from within the reservoir which is kept at a constant

temperature [7]. Our reservoir served only to neglect the effect of gravity on the sample exiting the die, the only place where measurements were made. When the plunger reached the programmed termination point, it retracted to the park position, the results (viscosity, shear rate, shear stress, and force) were printed, and the process could be repeated. The first run was used to clear the barrel of any possible material and then subsequent runs were recorded. For this study, each run was repeated four times, in order to average out deviations and provide reproducible results.

2.3 Dynamic Mechanical Data

The complex viscosity data (including G' , G'' , and $\tan \delta$) was collected using a Rheometrics Mechanical Spectrometer RMS-800 at the Polymer Processing Institute in Hoboken, NJ. Once again the material was dried and then compressed into disks with radius 12.5 mm (to match the radius of the spectrometer plates) and height of 1 mm (\pm 0.1 mm). The system was programmed to perform frequency sweeps within the range of 0.1 rad/s to 100 rad/s at a temperature of 290 °C and 280 °C. The material was then loaded between parallel plates as shown in Fig. 2.2, and the system was enclosed within a nitrogen atmosphere to minimize material degradation. Once the material and plates reached the desired temperature, the program was started and data was collected using an IBM compatible PC. The bottom plate was rotated at a given frequency yielding a sinusoidal strain and the top plate recorded the torque produced by the material. The data collected was frequency, storage and loss modulus, complex viscosity, and torque for both materials.

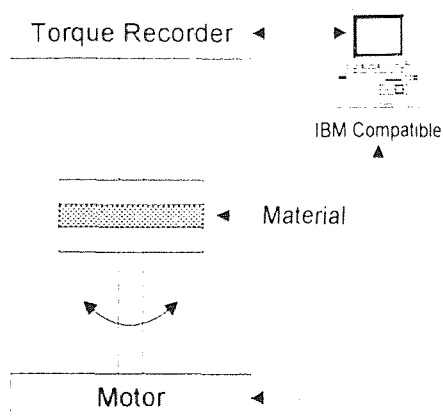


Figure 2.2 Mechanical Spectrometer Schematic

2.4 Modeling

Data handling and manipulation was done using Microsoft Excel 7.0 except for viscosity and extrudate swell modeling. The viscosity data was modeled on Matlab 4.2 by The Mathworks, Inc. using several models, including the Carreau and Cross models. The power-law index was calculated from the slope of the viscosity-shear rate curve and then used in the models. A least squares fit to minimize the error was performed on the data and fitted to yield a zero shear rate viscosity and characteristic time constant (computer code can be found in Appendix E). The viscosity data was then fitted to the Arrhenius expression to provide an activation energy as a measure of the temperature dependence. An activation energy was also calculated for the extrudate swell but no further modeling was done due to the lack of exit pressure drop data.

CHAPTER 3

THEORY

The theory described hereafter assumes a basic understanding of rheology. Concepts such as shear rate, and shear stress can be found in any rheology or polymer text.

3.1 Capillary Data

Because this study deals with two types of viscosity, we first define viscosity as shear stress divided by shear rate. Since both properties change depending on where the measurement is taken, we define our viscosity as the shear stress at the wall divided by the shear rate at the wall.

$$\eta \equiv \frac{\sigma}{\dot{\gamma}} \quad \text{or} \quad \eta \equiv \frac{\sigma_w}{\dot{\gamma}_w} \quad (1)$$

The capillary rheometer measures the force used to calculate the shear stress experienced by the material. The shear rate is set and can be calculated using Equation 2. But this shear rate is the apparent shear rate measured at the wall which assumes a Newtonian fluid.

$$\dot{\gamma}_a = \frac{4Q}{\pi R^3} \quad (2)$$

To account for the pseudoplastic fluid behavior, the Rabinowitsch correction factor must be applied to the capillary data, which is the bracket term in Equation 3. This now gives us the true shear rate at the wall, used later to find the true viscosity.

$$\dot{\gamma}_w = \frac{4Q}{\pi R^3} \left(\frac{3}{4} + \frac{1}{4} \frac{d \ln \dot{\gamma}_a}{d \ln \sigma_w} \right) \quad (3)$$

The Rabinowitsch correction factor accounts for the fact that the shear rate at the wall is greater for pseudoplastic fluids than for Newtonian fluids for a given volumetric flow rate [13].

3.2 Dynamic Mechanical Data

Assume a sinusoidal strain is applied to a material, the resulting stress would then also be sinusoidal. For a purely elastic material the stress would be in phase with the strain, but for a purely viscous materials, the stress would be 90° out of phase. Polymeric materials exhibit intermediate behavior and thus are described as viscoelastic [14]. One can then define a storage modulus which is the shear stress divided by the shear strain of the in-phase components (Equation 4) and a loss modulus with the out-of-phase components (Equation 5). Note: The term after the second = sign in the following equations is how the property was measured and will be described later.

$$G' \equiv \frac{\sigma'}{\gamma'} = K \left[\text{Real } M/\theta \right] \quad (4)$$

$$G'' \equiv \frac{\sigma''}{\gamma''} = K \left[\text{Imaginary } M/\theta \right] \quad (5)$$

G' and G'' are thought of as projections of a vector G^* that rotate in the complex plane, representing the in-phase and out-of-phase parts of G^* . G^* can then be defined in complex notation as:

$$G^* \equiv G' + iG'' = \sqrt{G'^2 + G''^2} \quad (6)$$

One can then define complex viscosity such as the one for capillary flow, but in terms of the in-phase and out-of-phase properties [15]:

$$\eta^* \equiv \eta' - i\eta'' = \sqrt{\eta'^2 + \eta''^2} = \dot{G} / \omega \quad (7)$$

Back calculating, we can then define the real and imaginary part of our complex viscosity, as shown in Equation 8.

$$\eta' = \frac{G''}{\omega} \quad \text{and} \quad \eta'' = \frac{G'}{\omega} \quad (8)$$

The apparatus used to apply a sinusoidal strain was discussed in the experimental chapter, and how it calculated the values will be discussed here. Torque (M) and the shearing angle (θ) are measured while the frequency (ω) is set. As shown in Equation 4, the storage modulus is found by taking the in-phase part of torque divided by shearing angle and multiplying it by a correction factor K. K, shown in Equation 9, depends on the height (distance between the 2 plates), and on the radius of the plate.

$$K = \frac{980.7(2H)}{10\pi\left(\frac{R}{10}\right)^4} \quad (9)$$

The loss modulus is found the same way as the storage modulus, but using the out-of-phase part. The complex modulus is calculated by squaring both terms and taking the square root, shown in Equation 6. The complex viscosity is just the complex modulus divided by the frequency at which the readings were taken at (Equation 7).

Although the complex viscosity is a measure of the resistance to flow, it is not the same as the viscosity measured by the capillary rheometer. One is measured as a function of shear rate while the other is with frequency. To be able to compare and utilize both, we can invoke the Cox-Merz Rule [16]:

$$|\eta^*(\omega)| = \sqrt{\eta'(\omega)^2 + \eta''(\omega)^2} = \eta(\dot{\gamma}) \Big|_{\dot{\gamma}=\omega} \quad (10)$$

Simply stated, the Cox-Merz rule predicts that the magnitude of the two data sets should be compared at equal values of the frequency and shear rate.

3.3 Data Analysis

Non-Newtonian behavior is described by the left side of Equation 11, known as the power law [17]. By dividing by the shear rate, we define viscosity as a function of shear rate, shown on the right. Therefore, if one were to plot shear rate versus viscosity on a log-log plot, the slope would be equal to 1-n. The power law index, n, is used in modeling viscosity (described later) and to compare degrees of non-Newtonian behavior.

$$\sigma = K(\dot{\gamma})^n \rightarrow \eta = K|\dot{\gamma}|^{n-1} \quad (11)$$

Since viscosity is temperature dependent, one can assume that the dependence can be modeled using an Arrhenius type equation, shown in Equation 12 [18].

$$\eta = A \exp\left(\frac{E_{\dot{\gamma}}}{RT}\right) \quad (12)$$

By taking the natural log of Equation 12, we get Equation 13, which appears to be of the form $y = mx + b$. By plotting $1/T$ vs. $\ln \eta$ the slope of the resulting curve is the activation energy divided by R_g , the gas constant.

$$\ln \eta = \ln A + \frac{E_{\dot{\gamma}}}{R} \frac{1}{T} \quad (13)$$

The activation energy is just a means by which one can compare the temperature dependence of a property of one material or condition to another. In this case, we use

viscosity to determine the activation energy of viscous flow. Because the extrudate swell is also temperature dependent, one should also be able to determine an activation energy of melt elasticity or extrudate swell. Therefore the same principles can also be applied to extrudate swell as applied to viscosity.

Although there has been some work in modeling and predicting die swell, no models were found that could accurately fit the experimental data and did not require pressure data and extensive calculations. Khalik, Hassager, and Bird [19] developed an extrudate model based on the normal stress function, calculated from viscosity data. Although the model displayed the general trend of die swell (Figure 3.1 [20]), it did model the experimental data very poorly.

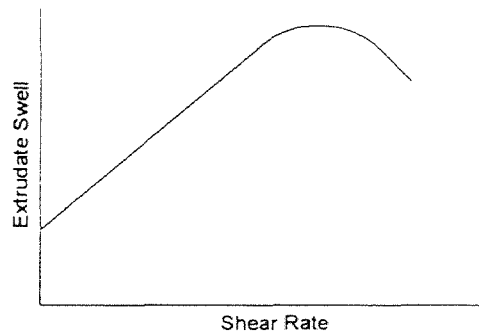


Figure 3.1 General Extrudate Swell Curve

Other equations, such as those developed by J. Z. Liang [21, 22], require pressure data that is unavailable in this study. Although Liang's study modeled the extrudate swell very

well, it could only be used for short dies (he used $D = 0.78$ mm and $L/D = 0.256$) where as our die was $D = 1.046$ mm and $L/D = 15$.

None of the models included predictions for critical shear or melt fracture, which played an important part in our study. The critical shear is the point of the onset of visible melt fracture. This critical shear introduces a discontinuity in the flow curves and various irregularities (spiraling, ripples, and bambooning) in the exiting extrudate. The instability is believed to be caused by the die entrance zone, where the flow lines are disturbed [23]. The perturbation and stagnation zones increase in importance as the shear rate increases until such time the stress imposed on the material exceeds its resistance and the material "ruptures". Although it is believed that the critical shear rate occurs just after reaching the maximum extrudate swell, this study found that it occurred just before reaching the maximum extrudate swell. But many factors are involved in the value of the critical shear rate, including die dimensions, entrance geometry, temperature, and material.

3.4 Modeling

Although there are many functions developed for viscosity modeling, for this study six were chosen: Bueche-Harding, Eyring, Carreau, Cross, Sutterby, and Vinogradov. All the models include a limiting viscosity, η_{∞} , at high shear rate which has been set to 0 resulting in the following models [24]:

$$\frac{\eta}{\eta_0} = \left[1 + (\dot{\tau}\dot{\gamma})^{0.75} \right]^{-1} \quad (\text{Bueche-Harding}) \qquad \frac{\eta}{\eta_0} = \frac{\sinh^{-1}(\dot{\tau}\dot{\gamma})}{\dot{\tau}\dot{\gamma}} \quad (\text{Eyring})$$

$$\frac{\eta}{\eta_0} = \left[\frac{\sinh^{-1}(\tau\dot{\gamma})}{\tau\dot{\gamma}} \right]^{1-n} \quad (\text{Sutterby}) \qquad \frac{\eta}{\eta_0} = \left[1 + (\tau\dot{\gamma})^{1-n} \right]^{-1} \quad (\text{Cross})$$

$$\frac{\eta}{\eta_0} = \left[1 + (\tau\dot{\gamma})^2 \right]^{(n-1)/2} \quad (\text{Carreau}) \qquad \frac{\eta}{\eta_0} = \left[1 + a(\tau\dot{\gamma})^{(1-n)/2} + (\tau\dot{\gamma})^{1-n} \right]^{-1} \quad (\text{Vinogradov})$$

They were chosen to cover a wide range of function types and their simplicity (no iterations required as with other systems). The first two are two parameter systems, while the Carreau, Cross, and Sutterby are three parameter models. The Vinogradov is the only four parameter model studied because it did not involve large computation time. Because the power-law index (n) was found using the method described earlier, only the zero-shear rate viscosity (η_0), the characteristic time constant (τ), and in the case of Vinogradov, the non-dimensional constant (a) needed to be calculated. The code used shown in Appendix E, with comments entered after any % symbol. The program starts by entering the experimental data, power-law index, type of model used, temperature desired, etc. and initializing a vector containing the initial guesses for the variables desired (η_0 , τ , and a). The vector is sent to a function called "fmins", along with all the data, which then returns the vector with the desired parameters. The function "fmins" minimizes an equation (written in a separate file called "fit", also found in Appendix E) using the data sent to it by changing the variables in the initial vector. The entire process performs a least-squares fit [25] on the data to match the model desired. In least-squares, the data is entered into the equation (as shown in Equation 14 using $y = mx + b$) and for each data set an error is calculated. The square of the errors are added together and this value is minimized by changing the parameter.

$$d_i = y_i - (mx_i + b)$$
$$s = d_1^2 + d_2^2 + d_3^2 + \dots + d_n^2 = \sum_{i=1}^n (y_i - mx_i - b)^2 \quad (14)$$

The values returned are then used in plotting the fitted line over the data and performing a regression on the data to find the coefficient of determination, R^2 [26].

CHAPTER 4

RESULTS

4.1 Viscosity

The raw data received from the rheometer can be found in Appendix A for the Shell 9506 PET and in Appendix B for the Sinco B PET. Data were taken at 270 °C, 280 °C, and 290 °C at varying shear rates from 134 s⁻¹ to 13340 s⁻¹. For each shear rate at a given temperature, there are four tables of values representing the force, shear stress, viscosity, and extrudate swell. There are four runs listed vertically, each divided into five zones, which correspond to the zones measured by the rheometer during testing. All the numbers have been averaged, except those that are highlighted because of their deviation from the norm. The extrudate swell calculations contain several measurements that were averaged for a single run and in the end combined with the other three runs.

Because the data collected is the apparent shear rate at the wall, the Rabinowitsch correction was calculated and applied. Since the apparent shear rate is determined using the properties of Newtonian fluids a large error can occur, especially at higher shear rates. Tables C-1 to C-3 in Appendix C show the Rabinowitsch calculations for Shell 9506 and Tables C-7 and C-8 contain the Sinco B calculations. Figure C-1 shows the shear rate-shear stress curves used in finding the correction factor for both materials. The shear stress is plotted on the x-axis because of the form of the Rabinowitsch Correction used requires the slope of the shear stress-shear rate curve. The data were fitted and the equations derived from the curves are found in Tables C-4 and C-9 for Shell 9506 and

Sinco B, respectively. From the curve equations, the slope of the shear rate-shear stress can be determined, as shown in the correction tables, and thus the Rabinowitsch correction factor. The apparent shear rate was increased by an average of 50% for the Shell 9506 and 25% for the Sinco B, with values ranging from 12% to 98% depending on the shear rate selected. The Sinco B average is lower since the material was not tested at higher shear rates because of melt flow instability. The Rabinowitsch Correction is a measure of how much a material deviates from Newtonian behavior. Once the shear rate was corrected, a new viscosity was calculated from the corrected shear rate. The viscosity/shear rate curve is therefore shifted to the right and down, corresponding to an increase in shear rate and decrease in viscosity (Fig. 4.1).

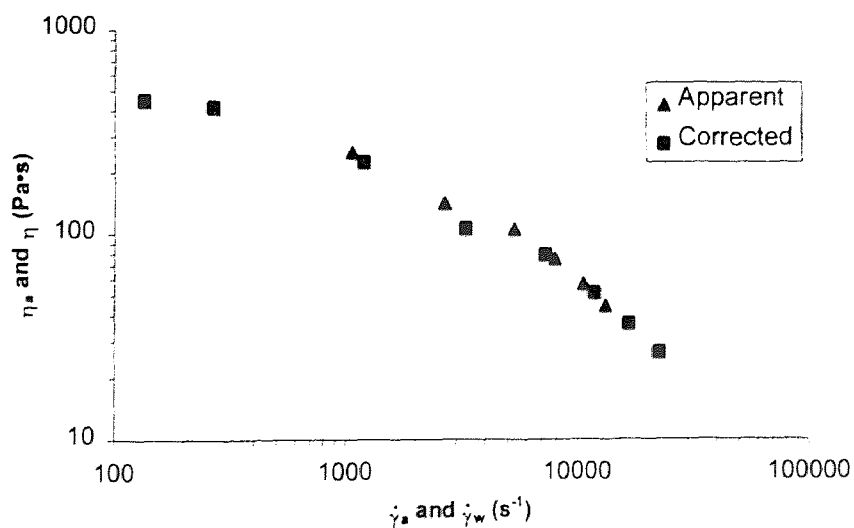


Figure 4.1 Viscosity vs. Shear Rate for Shell 9506 at 290 °C

The complete and corrected data is listed in Table C-5 for Shell 9506 and C-6 for Sinco B. The corrected shear rate/shear stress curves are found in Figures C-2 and C-3 for Shell 9506 and Sinco B respectively. At lower shear rates the shear stress values began to deviate from the previous trend and were therefore not included in the fitting. This was probably caused by the die of L/D of 15 which should be replaced by one with a smaller L/D in order to achieve the correct value. Since less material is being pushed through the die, a smaller die can be used so the measurements are not skewed by incorrect pressure drop readings.

As expected, the corrected viscosity of the Sinco B was also greater than the Shell 9506 as shown in Figure 4.2.

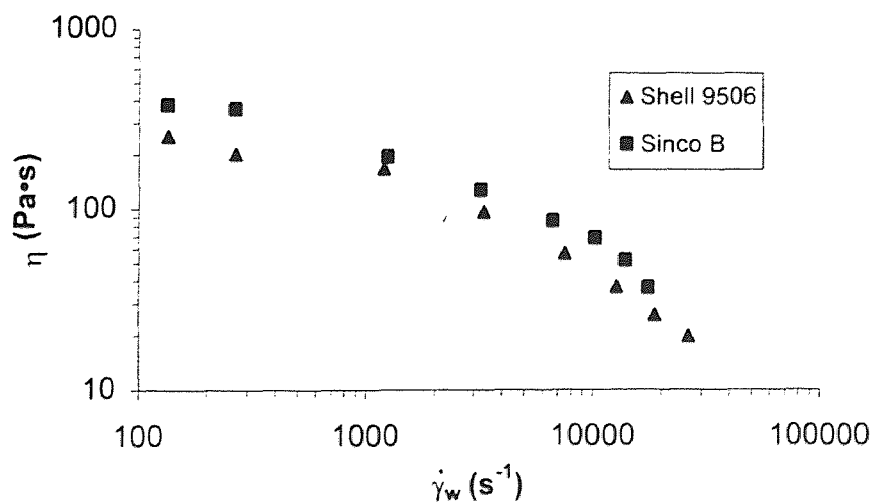


Figure 4.2 Viscosity vs. Shear Rate at 290 °C

Although not easy to see on a log-log scale, the Sinco B viscosity is 60% greater than the Shell 9506 at 290 °C and 40% at 280 °C, on average. Both curves seem to flatten out or tend toward Newtonian behavior near 100 s^{-1} and the power-law region within 2000 s^{-1} to 20000 s^{-1} . The capillary viscosity, including the complex viscosity, of both materials were fitted using viscosity models described in the modeling section.

4.2 Extrudate Swell

The extrudate swell measurements can also be found in Appendix A (Shell 9506) and Appendix B (Sinco B) for all shear rates and temperatures, except 134 s^{-1} at 270 °C. The extrudate swell is reported as both the swell ratio and swell % but most calculations were done using the swell ratio. The results are plotted in Figures C-4 and C-5 for Shell 9506 and Sinco B, respectively. The extrudate swell increases linearly for the Shell 9506 until reaching a plateau above $20,000 \text{ s}^{-1}$. At 290 °C the maximum swell ratio seems to be around 1.43 which is reached around $8,000 \text{ s}^{-1}$ while at 270 °C the maximum swell ratio is near 1.5, but is not achieved until well over $20,000 \text{ s}^{-1}$. Therefore, not only does the maximum extrudate swell increase with a decrease in temperature, but the critical shear rate increases. The die swell of Sinco B also increases with lower temperature but the critical shear rate decreases because of flow instability (see Figure C-5). In 1960, Beynon and Glyde [27] found that low density polyethylene had a maximum swell ratio that increased with temperature, the opposite that was found for PET. The fact that Shell 9506 is not branched could be one reason for this difference, but the Sinco B, which is presumably branched, also exhibits this difference.

The dashed line in Figure C-5 represents the approximate onset of melt fracture for Sinco B. Melt fracture was first determined visually, when fractures such as ripples and spirals appeared. Since one reading involved fracture while the one before it did not, the melt fracture is approximate because the exact point of melt fracture initiation is unknown. Almost no data was taken for Sinco B at 270 °C because of the immediate presence of melt fracture around 150 s⁻¹. The apparent branching increases the extrudate swell because the chains connecting the linear molecule expand, but they can also limit the maximum extrudate swell. The maximum swell would be limited to the size of the extended chains (due to disentanglement at high shear rates), showing why the extrudate swell seems to converge at higher shear rates for 290 °C and 280 °C. This could also explain the deviation from the results obtained by Beynon and Glyde [25] mentioned earlier.

Comparing the scales of Figures C-4 and C-5, one can see that the Sinco B material has a significantly larger extrudate swell than the Shell 9506. The maximum swell experienced by the Shell 9506 was 1.5 while the die swell of Sinco B passed 3.3, resulting in swell % of 50% and 232% respectively. The Shell 9506 also experienced no melt fracture except for a few readings at the highest shear rate at 270 °C. The Sinco experiences melt fracture quickly and doesn't show the linear swell-shear rate relationship at shear rates above 150 s⁻¹ at the temperatures used in this study. Figure 4.3 shows the extrudate swell for both materials at 290 °C, and illustrates the difference in swell ratios. On average, the extrudate swell of the Sinco is 2 times that of the Shell 9506 at 290 °C and 2.2 at 280 °C, ranging from 1.8 to 2.3.

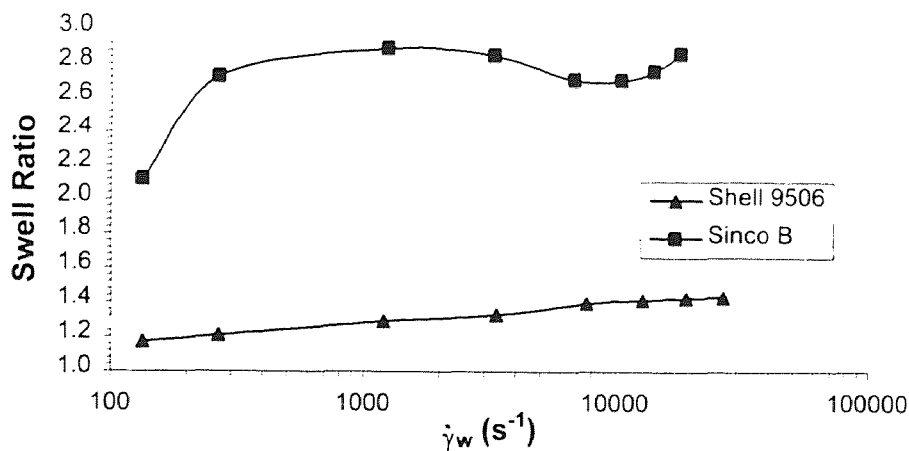


Figure 4.3 Extrudate Swell Ratio vs. Shear Rate at 290 °C

4.3 Activation Energy

The data used in the determination of the activation energy for viscous flow was taken from Table C-5, but the temperature was inverted and the logarithm of the viscosity was found. The calculated values allow Figure 4.4 to be plotted and the activation energy to be found from the slope of the lines, for a given shear rate. Except for the lines corresponding to the uncorrected shear rates $134 s^{-1}$ and $268 s^{-1}$, they all have a similar slope or activation energy. The activation energy for each shear rate is listed in Table C-10a and shown in graphical form in Figure 4.5. At high shear rates the activation energy seems to be relatively constant, while at low shear rates the trend appears to be linearly decreasing. Therefore, viscous flow is more dependent on temperature at low shear rates. One can then compare the importance of temperature not only between two shear rates, but also other materials at constant shear rates.

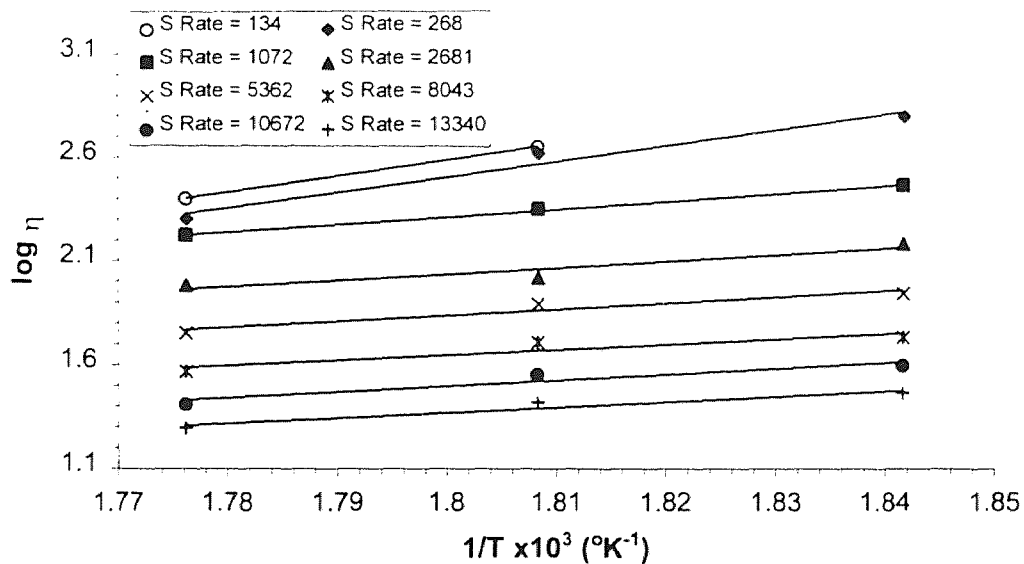


Figure 4.4 Determination of E_a of Melt Viscosity for Shell 9506

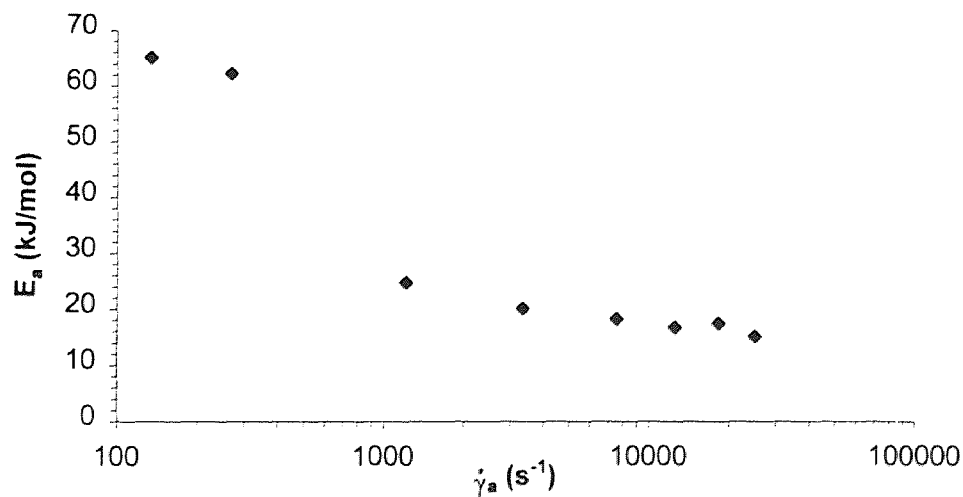


Figure 4.5 Activation Energy of Melt Viscosity vs. Shear Rate for Shell 9506

The concept of activation energy was also applied to the extrudate swell in order to measure the temperature dependence of melt elasticity. As before, the data used in the

calculations can be found in Table C-5 and the resulting values can be found in Table C-10b. Although the values found for the extrudate swell were lower than those found for viscosity, the trends of the data are alike. The extrudate swell behavior as a function of temperature is shown in Figure 4.6, similar to Figure 4.4 except for the magnitude of the y-axis (that is due to difference in properties measure, but the same trend applies). The activation energy of melt elasticity can then be shown as a function of shear rate in Figure 4.7, the same way it was shown for viscosity. The Arrhenius equation constant was not calculated for either property or material since it was not needed in this study.

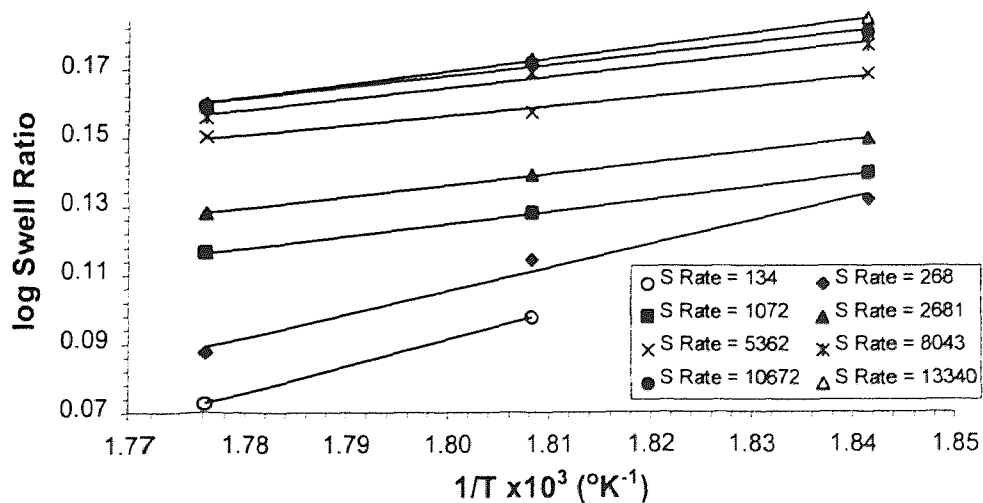


Figure 4.6 Determination of E_j of Melt Elasticity for Shell 9506

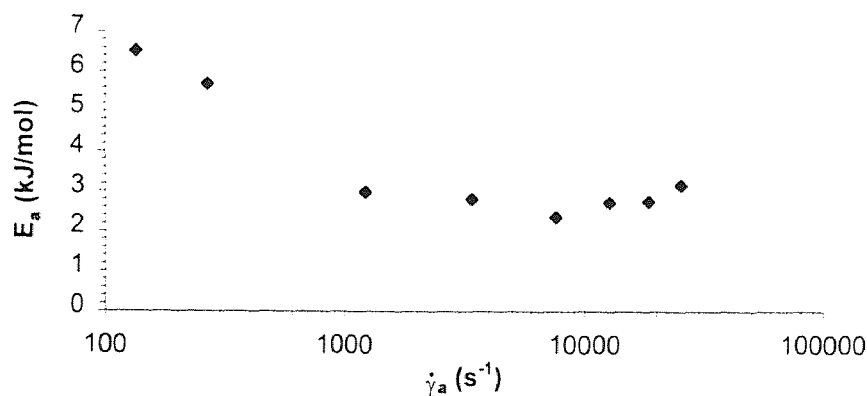


Figure 4.7 Activation Energy of Melt Elasticity vs. Shear Rate for Shell 9506

The trend shown in Figure 4.6 is the same as in Figure 4.4, except that the extrudate swell increases with respect to shear rate while the viscosity decreases. But as shown in Figures 4.5 and 4.7, both activation energies decrease linearly at low shear rates and eventually become constant at higher shear rates. The activation energy shown at 13340 s^{-1} was neglected because of trend deviation, probably due to measurement error at very high shear rates and the possibility of the onset of melt flow instability. No activation energy was calculated for the Sinco B because of lack of data at $270 \text{ }^\circ\text{C}$. The data collected at $290 \text{ }^\circ\text{C}$ and $280 \text{ }^\circ\text{C}$ are plotted versus the Shell 9506 at the same shear rates in Figures 4.8 and 4.9.

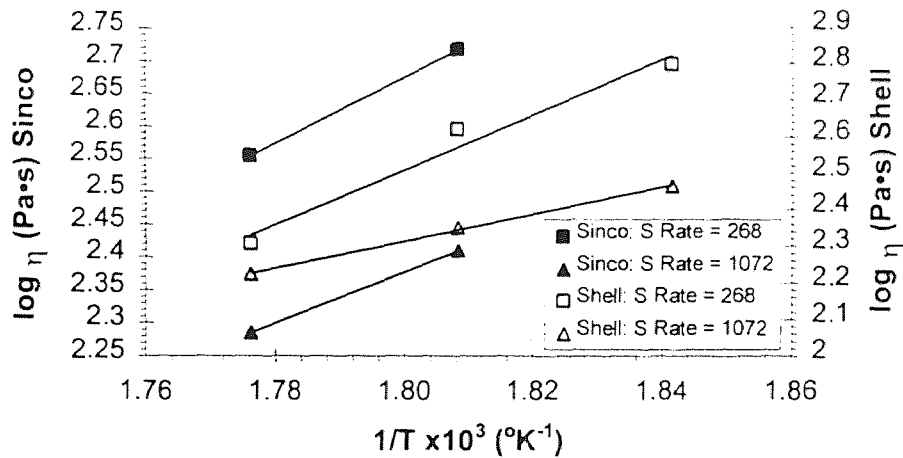


Figure 4.8 Comparison of E_{γ} of Melt Viscosity for Shell 9506 and Sinco B

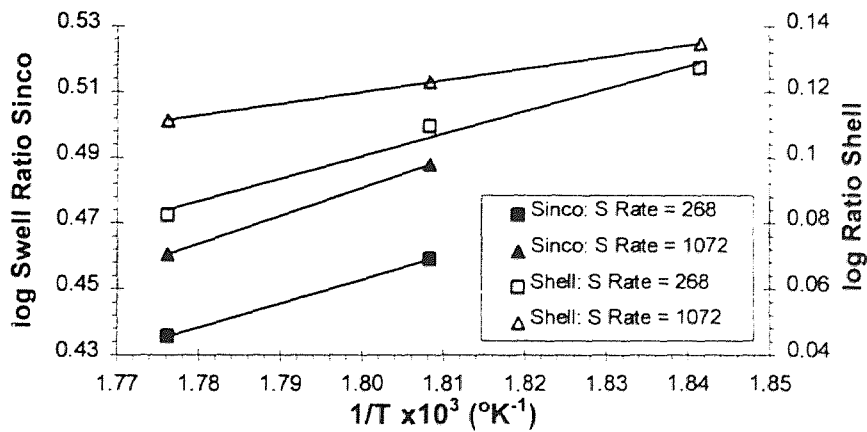


Figure 4.9 Comparison of E_{γ} of Melt Elasticity for Shell 9506 and Sinco B

The Sinco B material doesn't have the same scale values as the Shell 9506 but the trend is very similar. Thus the activation energies should be relatively close (they seem to be a little higher for the Sinco B, but without further analysis one cannot be sure) but the dependence on shear rate is unknown.

4.4 Complex Viscosity Determination

The complex viscosity was calculated as a supplement to the capillary viscosity measurements. Since the lower shear rates had larger errors due to material degradation within the barrel, complex viscosity data was used for the lower shear rate range. The data was then combined to produce Figures 4.10 (Shell 9506) and Figure 4.11 (Sinco B).

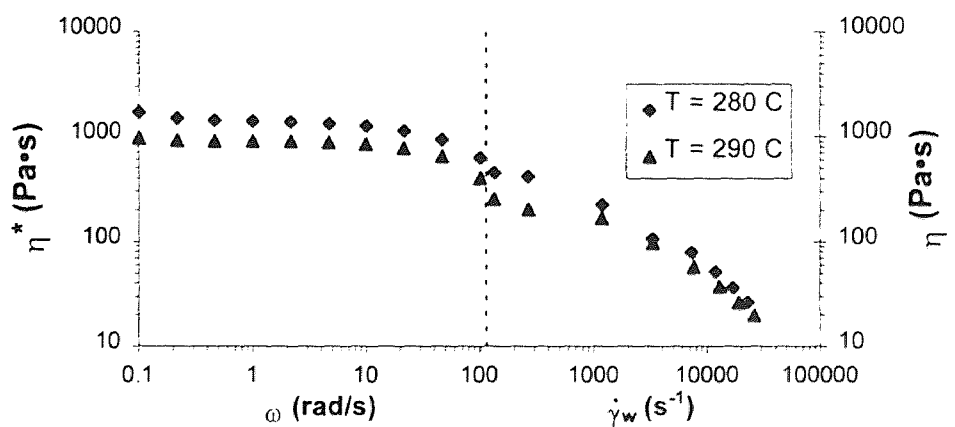


Figure 4.10 Complete Viscosity Curve for Shell 9506

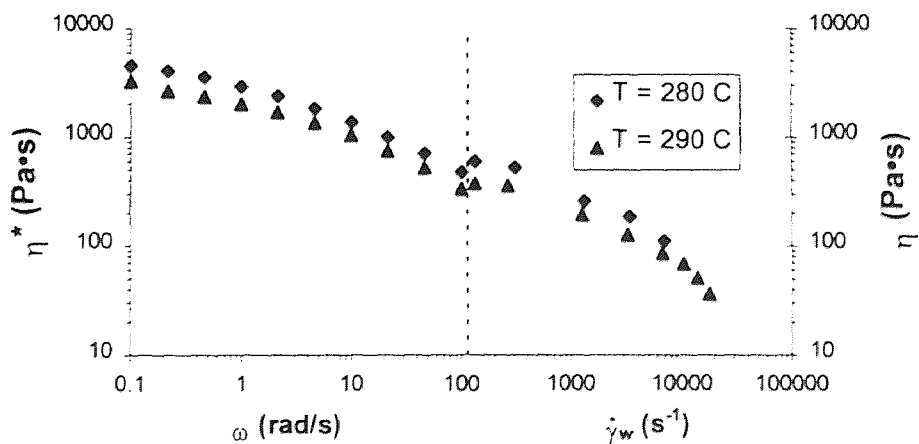


Figure 4.11 Complete Viscosity Curve for Sinco B

The complex viscosity data are in good agreement with the capillary viscosity data except around the 100 s^{-1} area. This is most likely due to the degradation of the capillary material at low shear rates as mentioned earlier. Degradation in the complex viscosity measurements was kept to a minimum because of the N_2 atmosphere used. The data from the four complex viscosity runs can be found in Tables C-11 and C-12, including G' , G'' , and torque measurements. Upon comparing the complete viscosity data for Shell 9506 and Sinco B (Figure 4.12), one notices that the complex viscosity of the materials cross at 20 s^{-1} .

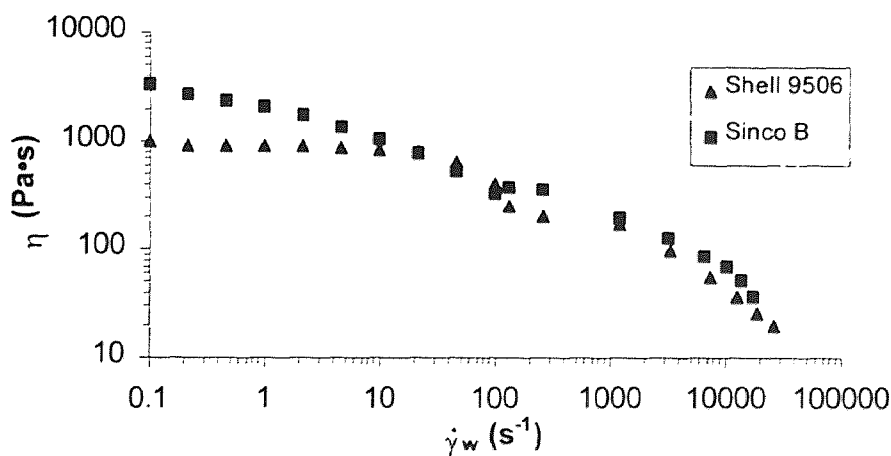


Figure 4.12 Viscosity vs. Shear Rate at $290 \text{ }^\circ\text{C}$ (Complete Curve)

The Sinco B viscosity is greater than the Shell 9506, except within the region of 20 s^{-1} to 100 s^{-1} . Since the Sinco B viscosity before and after the region is above the Shell 9506, one can speculate that the Sinco B viscosity remains above the Shell 9506 throughout (the reason of material degradation also aids in this assumption). The Shell

9506 data is Newtonian for shear rates smaller than 20 s^{-1} and then behaves as a power-law fluid at all shear rates above that. On the other hand, the Sinco B seems to behave entirely as a power-law fluid and never really reaches a Newtonian behavior. This broad power-law region is presumably caused by the branching present within the polymer and broad molecular weight distribution, typical of recycled material. At low shear rates the polymer becomes very entangled and as the shear rate increases the polymer disentangles eventually aligning and giving little resistance to flow [28]. The Sinco B material already has a high degree of entanglement and when it attempts aligns, it is hindered to align completely by branching. Thus, resulting in an almost totally pseudoplastic behavior until it eventually begins to degrade at extremely high shear rates.

Another measure of melt elasticity is G' , the storage modulus or the in-phase component discussed earlier. Comparing G' of both materials, as shown in Figure 4.13, leads to the same conclusion as with extrudate swell. The G' of Sinco B is larger than Shell 9506 by a factor of 10 at low frequencies and begin to converge as frequency increases. At low shear rates, there are more entanglements and chain interactions play a more important role in melt strength (giving rise to higher storage modulus). Since the Sinco B material is branched, it stands to reason that its melt elasticity would be larger than the linear Shell 9506. As frequency increases, entanglements decrease and thus both materials converge showing the decrease in entanglement importance. One will also notice that the Shell 9506 G' has a relatively constant slope while the Sinco B slope decreases with increasing frequency. This behavior is due to the branching that attempts aligns itself at higher frequencies for the Sinco B. The Shell 9506 is a linear polymer that doesn't experience transition from severe entanglements to aligned structures.

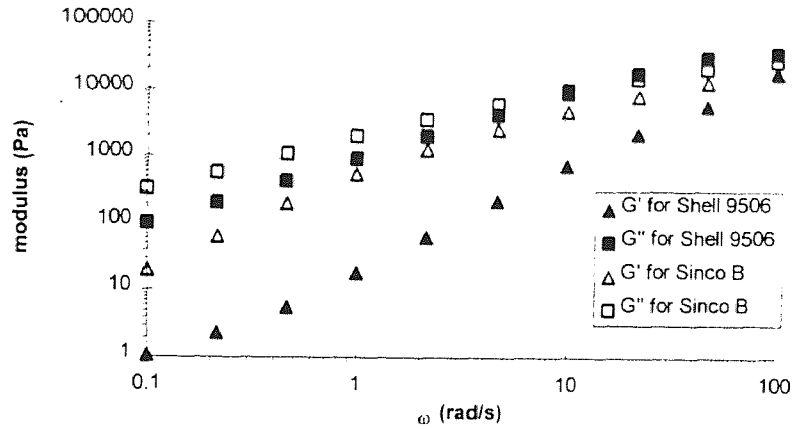


Figure 4.13 G' and G'' for Shell 9506 and Sinco B at 290 °C

4.5 Modeling

The first parameter that was determined was n , the power-law index using the average slope of the fully developed non-Newtonian capillary data. Figures D-1 to D-3 show the determination of n for Shell 9506 and Figure D-4 shows the data for Sinco B using Equation 11. The values were averaged over the temperature ranges and resulted in n being 0.29 for Shell 9506 and 0.49 for Sinco B. The data was then fitted using the six models and the power-law index using a least-squares fit procedure.

All the models used fitted the complete (capillary and complex) viscosity data well, but had a small problem describing the power-law region (Figures D-5 and D-6). The Newtonian region was modeled almost perfectly but the shape of the power-law region was modeled well but with some error (Figure 4.14). The error involved is small, but appears to be large due to the log-log scale used. Tables C-13 and C-14 list the coefficient of determination (R^2) for the models' fitting of both materials at 280 °C and

290 °C. The Shell 9506 is modeled best by the Cross, even though the Sutterby, Vinogradov, and Bueche-Harding models have higher R^2 . The last 3 models mentioned model the Newtonian data extremely well but appear to only model the power-law region shape and not the region. The Cross model models both regions very well and models the pseudoplastic region better than the rest, at the expense of the Newtonian region.

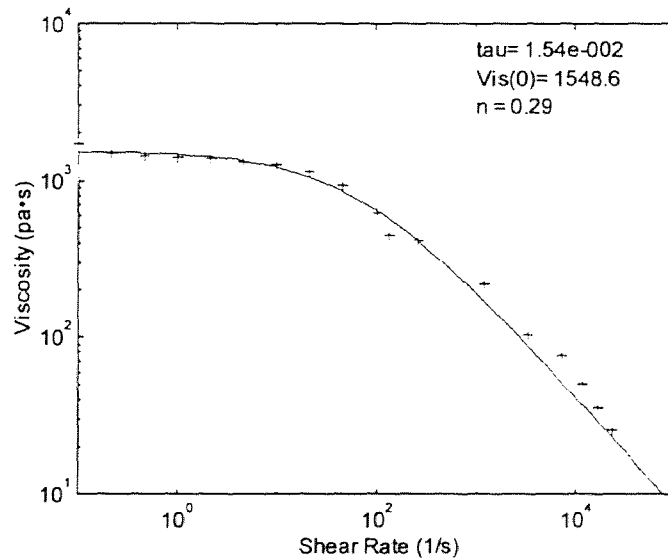


Figure 4.14 Cross Model of Shell 9506 at 280 °C

The data for Sinco B proved to be a more difficult because of the lack of a clear Newtonian region, which some models tried to plot (Figures D-6a to D-6f). Most models have been designed to include the power-law region, transition zone, and the Newtonian region. Models such as the Eyring and the Carreau tried to fit the data and included a transition zone and Newtonian region (Figures D-6b and D-6c), causing a drop in the quality of the fit, as shown by the R^2 values in Table C-14. The Cross and the Sutterby

were able to handle this change and model the Sinco B viscosity better than the Shell 9506 (Figures D-6d and D-6e). All the models experienced problems due to the discontinuity of the data caused by having 2 different types of viscosity. Neglecting the points with degradation error and the discontinuity, most of the models would have fitted the pseudoplastic region very well. The Vinogradov model experienced some problems involving the fourth parameter, a , which became negative for some of the data sets. Since this parameter should be positive, the Vinogradov model did not fit this data accurately. Similar results were obtained by Elbirli and Shaw in modeling LDPE and HDPE using similar models and methods [29]. They found that the best two parameter model was the Eyring, the Cross was the best three parameter model, and that the four parameter models did not increase precision in fitting.

CHAPTER 5

CONCLUSIONS

This study showed that materials with similar nominal IVs can rheologically differ significantly, leading to property misinterpretation. The melt viscosity, determined by capillary and dynamic rheometry, differ by an average of 61 % while the extrudate swell differ by 110%. Using melt viscosity as a guide for melt elasticity would clearly lead to miscalculations. Some other measure for melt strength should be included with nominal IV for polymer users to be able to correctly gauge the polymer's ability to foam during extrusion. As mentioned earlier, properties such as extrudate swell and storage modulus, among others, provide a more accurate measure of melt elasticity.

Activation energy, a property not frequently used in polymer processing, was used to measure and correlate the temperature dependence of viscous flow and melt elasticity. The data from the Shell 9506 showed that temperature became more significant as shear rate decreased into the range used in most applications. The importance of temperature increases dramatically (by more than 300%) with decreasing shear rate. Because of thermal degradation, temperature dependence is usually monitored closely during polymer processing. Activation energy could be used as a representative quantity to compare several materials and their response to temperature ranges within a process.

In modeling the melt viscosity data, the Cross model was found to fit the data the best for both systems. The Bueche-Harding and Eyring models did fairly well considering they were just two-parameter models. The Bueche-Harding modeled the Shell 9506 data very well because it assumes a power-law index of 0.25 and the parameter n of Shell 9506 was 0.29. The n for the Sinco B material was found to be 0.49 and thus was fitted poorly by the Bueche-Harding model (the Ferry model, which assumes an n of 0.5, could be used if one were interested in fitting the Sinco B melt viscosity only). Considering that the Vinogradov model was a four-parameter system, it modeled the data poorly for a more complex system. The increase in parameters and complexity by the Vinogradov model outweighs the little increase in data modeling accuracy provided.

Further study should be made in this area to provide more detail and information on the melt elasticity phenomenon of PET. In conjunction with this study, an analysis of unmodified recycled PET and modified virgin PET could provide further melt strength correlation. Foaming experiments, currently being investigated, should also provide valuable information on the processing aspects of melt elasticity and rheological properties that need to be quantified.

APPENDIX A

EXPERIMENTAL CAPILLARY DATA FOR SHELL 9506 PET

ID # = S19
 Speed = 0.5 in/min
 S Rate = 134 s⁻¹
 Temp = 290 °C

	Extrudate Swell (mm)				Viscosity (Pa*s)				
	Screen	Actual	Ratio	%	Zone 1	Zone 2	Zone 3	Zone 4	Zone 5
Run 1	90.0	1.20	1.15	14.7%	190.6	37.3	82.4	28.0	84.6
Run 2	90.2	1.20	1.15	14.9%	175.0	214.0	269.6	268.8	250.8
Run 3	93.0	1.24	1.18	18.5%	238.1	246.2	255.5	257.1	252.9
Run 4	93.6	1.25	1.19	19.2%	261.8	268.0	248.5	240.8	254.8
Average	91.7	1.22	1.17	16.8%	474.6	456.7	446.6	375.8	459.3
									252.8

	Force (lb _f)				Average	Shear Stress (kilodynes/cm ²)				
	Zone 1	Zone 2	Zone 3	Zone 4		Zone 5	Zone 1	Zone 2	Zone 3	Zone 4
Zone 1	24.5	4.8	10.6	3.6	10.9	256.2	50.1	110.8	37.6	113.7
Zone 2	22.5	27.5	38.5	38.4	34.8	235.2	287.5	462.6	401.5	383.9
Zone 3	30.8	35.5	36.7	36.9	36.4	319.9	371.2	383.1	385.8	380.0
Zone 4	37.5	38.3	35.8	34.8	36.6	342.1	400.5	374.3	363.9	370.2
Zone 5	61.0	58.7	57.4	48.3	59.0	637.9	613.8	600.2	505.0	617.3
					35.9					378.0

ID # = S11
 Speed = 1 in/min
 S Rate = 268 s⁻¹
 Temp = 290 °C

	Extrudate Swell (mm)				Viscosity (Pa*s)				
	Screen	Actual	Ratio	%	Zone 1	Zone 2	Zone 3	Zone 4	Zone 5
Run 1	98.3	1.31	1.25	25.3%	270.0	328.7	291.8	177.4	296.8
Run 2	92.3	1.23	1.18	17.6%	236.4	178.2	218.2	168.0	200.2
Run 3	94.8	1.26	1.21	20.7%	196.1	202.7	233.4	162.6	198.7
Run 4	94.0	1.25	1.20	19.8%	220.2	187.5	221.3	180.1	202.3
Average	94.9	1.26	1.21	20.9%	200.7	185.9	221.3	204.2	203.0
									201.1

	Force (lb _f)				Average	Shear Stress (kilodynes/cm ²)				
	Zone 1	Zone 2	Zone 3	Zone 4		Zone 5	Zone 1	Zone 2	Zone 3	Zone 4
Zone 1	69.4	84.5	75.0	45.6	76.3	725.7	883.6	784.3	476.8	797.9
Zone 2	60.9	45.8	56.1	43.2	51.5	636.8	478.9	586.6	451.7	538.5
Zone 3	50.4	52.1	60.0	41.8	51.1	527.0	544.8	627.4	437.1	534.1
Zone 4	56.6	48.2	56.9	46.3	52.0	591.8	504.0	595.0	484.1	543.7
Zone 5	51.6	47.8	56.9	52.5	52.2	539.6	499.8	595.0	549.0	545.9
					51.7					540.5

ID # = S12
 Speed = 4 in/min
 S Rate = 1072 s⁻¹
 Temp = 290 °C

	Extrudate Swell (mm)				Viscosity (Pa*s)					
	Screen	Actual	Ratio	%						
Run 1	101.0	1.35	1.29	28.7%	Zone 1	127.3	188.1	248.3	170.4	183.5
Run 2	101.8	1.36	1.30	29.6%	Zone 2	123.2	166.7	230.7	192.8	178.4
Run 3	101.3	1.35	1.29	29.0%	Zone 3	138.3	180.7	259.4	191.1	192.4
Run 4	101.5	1.35	1.29	29.3%	Zone 4	146.7	183.4	382.5	185.9	172.0
Average	101.4	1.35	1.29	29.2%	Zone 5	154.9	204.9	268.9	187.1	204.0
										186.0

	Force (lb _f)				Average	Shear Stress (kilodynes/cm ²)					
Zone 1	130.9	193.4	255.3	175.2	188.7	Zone 1	136.8	202.2	266.9	183.2	197.3
Zone 2	126.7	171.4	237.2	198.3	183.4	Zone 2	132.4	179.2	248.0	207.3	191.7
Zone 3	142.2	185.8	266.7	196.5	197.8	Zone 3	148.7	194.2	278.8	205.9	206.9
Zone 4	150.9	188.6	393.3	191.2	176.9	Zone 4	157.8	197.2	411.2	199.9	185.0
Zone 5	159.3	210.7	276.5	192.4	209.7	Zone 5	166.5	220.3	289.1	201.2	219.3
					191.3						200.0

ID # = S13
 Speed = 10 in/min
 S Rate = 2681 s⁻¹
 Temp = 290 °C

	Extrudate Swell (mm)				Viscosity (Pa*s)					
	Screen	Actual	Ratio	%						
Run 1	104.0	1.39	1.33	32.5%	Zone 1	115.4	107.1	867.6	54.4	111.3
Run 2	104.3	1.39	1.33	32.8%	Zone 2	119.2	128.8	109.5	186.7	119.2
Run 3	105.0	1.40	1.34	33.8%	Zone 3	134.0	143.8	114.9	104.8	124.4
Run 4	103.4	1.38	1.32	31.7%	Zone 4	132.0	194.3	156.6	117.6	124.8
Average	104.2	1.39	1.33	32.7%	Zone 5	121.5	129.9	110.2	104.1	116.4
										119.2

	Force (lb _f)				Average	Shear Stress (kilodynes/cm ²)					
Zone 1	296.6	275.4	22.3	1.4	286.0	Zone 1	310.1	287.9	233.1	14.6	299.0
Zone 2	306.5	331.2	281.6	4.8	306.4	Zone 2	320.5	346.3	294.4	50.1	320.4
Zone 3	344.5	369.8	295.4	269.4	319.8	Zone 3	360.2	386.7	308.9	281.7	334.4
Zone 4	339.3	499.6	402.7	302.3	320.8	Zone 4	354.8	522.4	421.1	316.1	335.5
Zone 5	312.5	334.1	283.3	267.6	299.4	Zone 5	326.7	349.3	296.2	279.8	313.0
					306.5						320.4

ID # = S15
 Speed = 20 in/min
 S Rate = 5362 s⁻¹
 Temp = 290 °C

	Extrudate Swell (mm)				Viscosity (Pa*s)					
	Screen	Actual	Ratio	%	Zone 1	Zone 2	Zone 3	Zone 4	Zone 5	Average
Run 1	110.0	1.47	1.40	40.2%	73.4	75.2	83.9	92.4	88.1	76.9
Run 2	109.7	1.46	1.40	39.7%	75.2	75.2	83.9	92.4	88.1	77.5
Run 3	109.3	1.46	1.39	39.3%	83.9	75.2	83.8	101.0	79.7	83.9
Run 4	109.7	1.46	1.40	39.7%	92.4	78.3	101.0	104.2	79.2	99.2
Average	109.7	1.46	1.40	39.7%	88.1	75.3	79.7	79.2		82.3
										80.2

	Force (lb _f)				Average	Shear Stress (kilodynes/cm ²)					
	Zone 1	Zone 2	Zone 3	Zone 4	Zone 5	Zone 1	Zone 2	Zone 3	Zone 4	Zone 5	Average
Zone 1	377.7	1.2	414.6	395.0	395.8	394.9	12.5	433.5	413.0	413.8	413.8
Zone 2	386.6	109.3	407.3	401.0	398.3	404.2	114.2	435.9	419.3	419.8	419.8
Zone 3	431.4	382.7	431.1	431.7	431.4	451.1	400.2	450.8	451.4	451.1	451.1
Zone 4	475.1	402.7	519.2	527.0	507.1	496.8	421.1	542.9	560.5	533.4	533.4
Zone 5	452.9	387.5	410.1	407.3	423.4	473.6	405.2	428.8	425.9	442.8	442.8
					412.2						431.9

ID # = S16
 Speed = 30 in/min
 S Rate = 8043 s⁻¹
 Temp = 290 °C

	Extrudate Swell (mm)				Viscosity (Pa*s)					
	Screen	Actual	Ratio	%	Zone 1	Zone 2	Zone 3	Zone 4	Zone 5	Average
Run 1	110.7	1.48	1.41	41.0%	56.7	58.0	59.5	63.0	63.4	57.1
Run 2	111.3	1.48	1.42	41.9%	58.0	58.0	59.5	63.0	63.4	57.5
Run 3	111.0	1.48	1.41	41.4%	59.5	53.2	59.1	62.4	59.8	59.1
Run 4	111.3	1.48	1.42	41.9%	63.0	60.9	64.2	62.4	59.0	62.6
Average	111.1	1.48	1.42	41.5%	63.4	58.4	59.8	59.0		60.2
										60.6

	Force (lb _f)				Average	Shear Stress (kilodynes/cm ²)					
	Zone 1	Zone 2	Zone 3	Zone 4	Zone 5	Zone 1	Zone 2	Zone 3	Zone 4	Zone 5	Average
Zone 1	437.7	0.6	437.9	446.7	440.8	457.7	6.2	457.9	467.1	460.9	460.9
Zone 2	447.6	6.3	445.4	438.6	443.9	468.0	65.8	465.7	458.6	464.1	464.1
Zone 3	459.2	410.4	456.4	452.7	456.1	480.2	429.1	477.2	473.4	476.9	476.9
Zone 4	485.9	469.8	495.5	481.2	483.1	508.1	491.2	518.1	503.2	505.2	505.2
Zone 5	489.3	451.0	461.7	455.5	464.4	511.6	471.6	482.8	476.3	485.6	485.6
					451.3						471.9

ID # = S17
 Speed = 40 in/min
 S Rate = 10672 s⁻¹
 Temp = 290 °C

	Extrudate Swell (mm)				Viscosity (Pa*s)				
	Screen	Actual	Ratio	%	Zone 1	Zone 2	Zone 3	Zone 4	Zone 5
Run 1	111.7	1.49	1.42	42.3%	41.1	41.2	40.7	41.3	41.1
Run 2	112.3	1.50	1.43	43.1%	41.6	42.8	42.4	42.3	42.3
Run 3	112.5	1.50	1.43	43.3%	43.3	44.6	44.8	45.3	44.5
Run 4	111.5	1.49	1.42	42.1%	46.1	47.7	47.2	47.8	47.2
Average	112.0	1.49	1.43	42.7%	44.7	44.3	43.2	44.6	44.2
									45.3

	Force (lb _f)				Average	Shear Stress (kilodynes/cm ²)				
	Zone 1	Zone 2	Zone 3	Zone 4	Zone 5	Zone 1	Zone 2	Zone 3	Zone 4	Zone 5
Zone 1	423.5	423.7	418.9	425.6	422.9	442.8	493.0	438.0	445.0	454.7
Zone 2	428.6	440.3	436.1	435.3	435.1	448.2	360.4	456.0	455.2	453.1
Zone 3	445.8	459.0	460.8	466.0	457.9	466.1	479.9	481.0	487.3	478.6
Zone 4	474.3	490.5	485.3	492.4	485.6	495.9	512.9	507.4	514.9	507.8
Zone 5	459.7	455.7	444.3	459.4	454.8	480.7	476.5	464.6	480.4	475.6
					466.1					487.3

ID # = S18
 Speed = 50 in/min
 S Rate = 13340 s⁻¹
 Temp = 290 °C

	Extrudate Swell (mm)				Viscosity (Pa*s)				
	Screen	Actual	Ratio	%	Zone 1	Zone 2	Zone 3	Zone 4	Zone 5
Run 1	112.7	1.50	1.44	43.6%	38.5	37.7	33.0	36.5	37.6
Run 2	112.0	1.49	1.43	42.7%	38.5	38.4	38.2	37.3	38.1
Run 3	112.3	1.50	1.43	43.1%	39.7	39.1	40.3	37.9	39.3
Run 4	111.7	1.49	1.42	42.3%	41.2	41.1	42.0	39.7	40.7
Average	112.2	1.50	1.43	42.9%	40.0	37.9	38.2	38.2	38.6
									38.6

	Force (lb _f)				Average	Shear Stress (kilodynes/cm ²)				
	Zone 1	Zone 2	Zone 3	Zone 4	Zone 5	Zone 1	Zone 2	Zone 3	Zone 4	Zone 5
Zone 1	495.6	485.4	425.3	470.1	483.7	518.2	507.6	444.7	491.6	505.8
Zone 2	495.6	494.4	491.9	480.4	490.6	518.2	517.0	514.4	502.3	513.0
Zone 3	510.8	502.7	518.2	488.3	505.0	534.1	525.6	541.9	510.6	528.1
Zone 4	529.8	529.2	540.8	510.1	523.0	554.0	553.4	565.5	533.9	547.1
Zone 5	514.4	487.0	491.5	492.1	496.3	537.9	509.4	513.9	514.6	519.0
					497.3					522.6

ID # = S29
 Speed = 0.5 in/min
 S Rate = 134 s⁻¹
 Temp = 280 °C

	Extrudate Swell (mm)				Viscosity (Pa•s)				
	Screen	Actual	Ratio	%	Zone 1	Zone 2	Zone 3	Zone 4	Zone 5
Run 1	97.0	1.29	1.24	23.6%	343.1	39.6	26.4	40.4	35.5
Run 2	97.2	1.30	1.24	23.8%	390.8	402.3	410.1	276.2	401.1
Run 3	97.1	1.30	1.24	23.8%	399.6	435.0	418.6	440.4	431.3
Run 4	97.3	1.30	1.24	23.9%	401.3	405.4	413.2	441.2	415.3
Average	97.1	1.30	1.24	23.8%	576.6	544.7	550.1	632.6	557.1
									451.2

	Force (lb _f)				Average	Shear Stress (kilodynes/cm ²)				
	Zone 1	Zone 2	Zone 3	Zone 4	Zone 5	Zone 1	Zone 2	Zone 3	Zone 4	Zone 5
Zone 1	44.1	5.1	3.4	5.2	4.6	461.1	53.3	35.5	54.0	47.6
Zone 2	43.8	51.7	52.7	35.5	49.4	458.0	540.6	551.1	371.2	516.6
Zone 3	47.5	55.9	53.8	56.6	55.4	496.7	584.5	562.6	591.8	579.6
Zone 4	49.0	52.1	53.1	56.7	52.7	512.4	544.8	555.2	592.9	551.3
Zone 5	74.1	70.0	70.7	81.3	71.6	774.8	732.0	739.3	850.1	748.7
					57.3					599.1

ID # = S27
 Speed = 1 in/min
 S Rate = 268 s⁻¹
 Temp = 280 °C

	Extrudate Swell (mm)				Viscosity (Pa•s)				
	Screen	Actual	Ratio	%	Zone 1	Zone 2	Zone 3	Zone 4	Zone 5
Run 1	101.0	1.35	1.29	28.7%	338.1	324.1	467.3	NA	376.5
Run 2	101.8	1.36	1.30	29.6%	281.3	367.3	442.7	NA	405.0
Run 3	100.5	1.34	1.28	28.0%	350.1	391.0	418.2	NA	404.6
Run 4	100.7	1.34	1.28	28.3%	346.6	435.0	436.9	NA	436.0
Average	101.0	1.35	1.29	28.7%	413.2	477.8	485.5	NA	481.7
									415.2

	Force (lb _f)				Average	Shear Stress (kilodynes/cm ²)				
	Zone 1	Zone 2	Zone 3	Zone 4	Zone 5	Zone 1	Zone 2	Zone 3	Zone 4	Zone 5
Zone 1	NA	NA	NA	NA	NA	NA	NA	NA	NA	NA
Zone 2	NA	NA	NA	NA	NA	NA	NA	NA	NA	NA
Zone 3	NA	NA	NA	NA	NA	NA	NA	NA	NA	NA
Zone 4	NA	NA	NA	NA	NA	NA	NA	NA	NA	NA
Zone 5	NA	NA	NA	NA	NA	NA	NA	NA	NA	NA
					NA					NA

ID # = S26
 Speed = 4 in/min
 S Rate = 1072 s⁻¹
 Temp = 280 °C

	Extrudate Swell (mm)			
	Screen	Actual	Ratio	%
Run 1	104.3	1.39	1.33	32.9%
Run 2	104.3	1.39	1.33	32.9%
Run 3	104.0	1.39	1.33	32.5%
Run 4	104.0	1.39	1.33	32.5%
Average	104.2	1.39	1.33	32.7%

	Viscosity (Pa*s)				
	Zone 1	260.0	260.8	256.0	239.2
Zone 2	227.6	203.6	240.2	286.5	223.8
Zone 3	281.5	247.2	263.9	272.2	272.5
Zone 4	325.6	299.4	309.0	332.0	322.2
Zone 5	310.5	253.1	257.4	240.8	250.4
					251.4

	Force (lb _f)				Average
	Zone 1	267.3	268.2	263.2	246
Zone 2	234.0	209.4	247.0	294.6	230.1
Zone 3	289.4	254.2	271.4	279.9	280.2
Zone 4	324.8	307.8	317.7	341.4	328.0
Zone 5	319.3	260.2	264.7	247.6	257.5
					258.5

	Shear Stress (kilodynes/cm ²)				
	Zone 1	279.5	280.4	275.2	257.2
Zone 2	244.7	218.9	258.2	308.0	240.6
Zone 3	302.6	265.8	283.8	292.7	293.0
Zone 4	350.1	321.8	332.2	357.0	346.4
Zone 5	333.9	272.1	276.8	258.9	269.3
					270.3

ID # = S21
 Speed = 10 in/min
 S Rate = 2681 s⁻¹
 Temp = 280 °C

	Extrudate Swell (mm)			
	Screen	Actual	Ratio	%
Run 1	106.5	1.42	1.36	35.7%
Run 2	106.7	1.42	1.36	35.9%
Run 3	107.3	1.43	1.37	36.8%
Run 4	107.0	1.43	1.36	36.3%
Average	106.9	1.43	1.36	36.2%

	Viscosity (Pa*s)				
	Zone 1	77.0	120.6	122.0	126.5
Zone 2	88.3	123.4	119.7	119.8	119.8
Zone 3	97.6	138.6	131.0	134.7	134.8
Zone 4	113.7	187.6	139.9	156.6	148.3
Zone 5	116.3	146.8	117.0	124.9	119.4
					141.5

	Force (lb _f)				Average
	Zone 1	197.9	310.0	313.7	325.3
Zone 2	227.0	317.2	307.8	308	311.0
Zone 3	251.0	356.4	336.7	346.3	346.5
Zone 4	292.3	482.3	359.6	402.6	381.1
Zone 5	299.0	377.5	300.8	321.2	307.0
					320.2

	Shear Stress (kilodynes/cm ²)				
	Zone 1	206.9	324.1	328.0	340.1
Zone 2	237.3	331.7	321.8	322.0	325.2
Zone 3	262.4	372.7	352.1	362.1	362.3
Zone 4	305.6	504.3	376.0	421.0	398.5
Zone 5	312.6	394.7	314.5	335.8	321.0
					347.5

ID # = S22
 Speed = 20 in/min
 S Rate = 5362 s⁻¹
 Temp = 280 °C

	Extrudate Swell (mm)			
	Screen	Actual	Ratio	%
Run 1	113.8	1.52	1.45	44.9%
Run 2	110.7	1.48	1.41	41.0%
Run 3	109.5	1.46	1.40	39.5%
Run 4	112.3	1.50	1.43	43.0%
Average	111.5	1.49	1.42	42.1%

	Viscosity (Pa*s)				
	Zone 1	82.7	106.5	99.1	104.8
Zone 2	87.4	104.1	103.2	105.6	104.3
Zone 3	106.4	110.1	104.6	105.9	105.6
Zone 4	115.3	122.7	114.3	116.0	115.2
Zone 5	135.4	131.8	121.2	107.6	129.5
					105.2

	Force (lb _f)				Average
	Zone 1	425.1	563.0	509.6	557.7
Zone 2	449.6	535.6	530.6	543.0	536.4
Zone 3	541.8	566.3	548.0	560.1	554.1
Zone 4	592.9	631.2	587.9	596.5	592.4
Zone 5	696.0	677.6	623.1	553.5	665.6
					560.8

	Shear Stress (kilodynes/cm ²)				
	Zone 1	443.5	588.7	532.9	583.2
Zone 2	470.1	760.0	554.8	567.8	561.3
Zone 3	566.5	592.2	573.0	585.7	575.1
Zone 4	620.0	660.0	614.7	623.7	619.5
Zone 5	727.8	708.5	651.6	578.8	696.0
					574.1

ID # = S23
 Speed = 30 in/min
 S Rate = 8043 s⁻¹
 Temp = 280 °C

	Extrudate Swell (mm)			
	Screen	Actual	Ratio	%
Run 1	114.5	1.53	1.46	45.9%
Run 2	114.7	1.53	1.46	46.1%
Run 3	114.7	1.53	1.46	46.1%
Run 4	114.3	1.52	1.46	45.6%
Average	114.5	1.53	1.46	45.9%

	Viscosity (Pa*s)				
	Zone 1	75.1	77.1	75.3	76.7
Zone 2	72.9	76.0	74.3	75.4	75.2
Zone 3	74.9	75.9	76.8	75.9	75.9
Zone 4	79.6	87.8	81.9	84.7	82.1
Zone 5	77.0	77.9	76.8	76.1	77.0
					75.6

	Force (lb _f)				Average
	Zone 1	579.8	594.5	580.6	591.7
Zone 2	562.3	586.4	573.6	581.8	580.6
Zone 3	578.1	600.7	592.2	585.4	589.1
Zone 4	614.5	677.3	632.1	653.6	633.4
Zone 5	594.1	600.8	592.9	586.9	593.7
					587.5

	Shear Stress (kilodynes/cm ²)				
	Zone 1	606.3	621.6	607.1	618.7
Zone 2	588.0	613.2	599.8	608.4	607.1
Zone 3	604.5	628.1	619.2	612.1	611.9
Zone 4	642.6	708.2	661.0	683.4	662.3
Zone 5	621.2	628.2	620.0	613.7	620.8
					608.6

ID # = S24
 Speed = 40 in/min
 S Rate = 10672 s⁻¹
 Temp = 280 °C

	Extrudate Swell (mm)				Viscosity (Pa•s)				
	Screen	Actual	Ratio	%	Zone 1	Zone 2	Zone 3	Zone 4	Zone 5
Run 1	115.0	1.53	1.47	46.5%	56.7	57.4	55.8	54.5	56.6
Run 2	115.3	1.54	1.47	46.8%	56.5	57.1	54.6	55.7	56.4
Run 3	115.5	1.54	1.47	47.2%	57.3	57.8	54.2	56.3	57.1
Run 4	115.7	1.54	1.47	47.4%	61.5	61.5	58.1	58.2	59.8
Average	115.4	1.54	1.47	47.0%	56.8	58.3	56.6	54.2	56.5
									56.7

	Force (lb _f)				Average	Shear Stress (kilodynes/cm ²)				
	Zone 1	Zone 2	Zone 3	Zone 4	Zone 5	Zone 1	Zone 2	Zone 3	Zone 4	Zone 5
Zone 1	583.9	590.7	574.0	561	582.9	610.6	617.7	600.2	586.6	609.5
Zone 2	581.4	587.6	561.5	572.7	580.6	607.9	614.4	587.1	598.8	607.0
Zone 3	589.2	594.9	557.7	578.9	587.7	616.1	622.1	583.2	605.3	614.5
Zone 4	632.3	633.1	597.4	598.9	615.4	661.2	662.0	624.7	626.2	643.5
Zone 5	581.2	600.0	582.2	557.6	580.3	610.9	627.4	608.8	583.1	615.7
					582.8					611.7

ID # = S25
 Speed = 50 in/min
 S Rate = 13340 s⁻¹
 Temp = 280 °C

	Extrudate Swell (mm)				Viscosity (Pa•s)				
	Screen	Actual	Ratio	%	Zone 1	Zone 2	Zone 3	Zone 4	Zone 5
Run 1	115.5	1.54	1.47	47.2%	44.5	44.3	43.7	43.6	44.1
Run 2	116.0	1.55	1.48	47.8%	44.5	44.4	49.5	43.0	44.0
Run 3	115.5	1.54	1.47	47.2%	45.9	45.7	43.7	44.1	44.9
Run 4	115.3	1.54	1.47	46.9%	48.7	43.2	49.9	46.9	48.5
Average	115.6	1.54	1.47	47.3%	45.6	43.2	44.6	43.7	44.3
									44.3

	Force (lb _f)				Average	Shear Stress (kilodynes/cm ²)				
	Zone 1	Zone 2	Zone 3	Zone 4	Zone 5	Zone 1	Zone 2	Zone 3	Zone 4	Zone 5
Zone 1	572.0	570.0	48.6	561.2	567.7	598.1	596.0	508.2	586.8	593.6
Zone 2	573.0	571.4	534.0	552.6	565.7	599.2	597.5	558.4	577.8	591.5
Zone 3	590.4	571.5	562.6	566.9	567.0	617.4	597.6	588.3	592.8	599.0
Zone 4	626.8	597.6	641.4	603.0	617.2	655.4	614.4	670.7	630.5	652.2
Zone 5	586.4	556.4	574.0	562.8	569.9	613.2	581.8	600.2	588.5	595.9
					567.6					595.0

ID # = S39
 Speed = 0.5 in/min
 S Rate = 134 s⁻¹
 Temp = 270 °C

	Extrudate Swell (mm)				Viscosity (Pa*s)					
	Screen	Actual	Ratio	%	Zone 1	Zone 2	Zone 3	Zone 4	Zone 5	Average
Run 1	NA	NA	NA	NA	NA	NA	NA	NA	NA	NA
Run 2	NA	NA	NA	NA	NA	NA	NA	NA	NA	NA
Run 3	NA	NA	NA	NA	NA	NA	NA	NA	NA	NA
Run 4	NA	NA	NA	NA	NA	NA	NA	NA	NA	NA
Average	NA	NA	NA	NA	NA	NA	NA	NA	NA	NA

	Force (lb _f)				Average	Shear Stress (kilodynes/cm ²)					
	Zone 1	Zone 2	Zone 3	Zone 4	Zone 5	Zone 1	Zone 2	Zone 3	Zone 4	Zone 5	Average
Zone 1	NA	NA	NA	NA	NA	NA	NA	NA	NA	NA	NA
Zone 2	NA	NA	NA	NA	NA	NA	NA	NA	NA	NA	NA
Zone 3	NA	NA	NA	NA	NA	NA	NA	NA	NA	NA	NA
Zone 4	NA	NA	NA	NA	NA	NA	NA	NA	NA	NA	NA
Zone 5	NA	NA	NA	NA	NA	NA	NA	NA	NA	NA	NA
					NA						NA

ID # = S37
 Speed = 1 in/min
 S Rate = 268 s⁻¹
 Temp = 270 °C

	Extrudate Swell (mm)				Viscosity (Pa*s)					
	Screen	Actual	Ratio	%	Zone 1	Zone 2	Zone 3	Zone 4	Zone 5	Average
Run 1	104.7	1.40	1.33	33.4%	613.5	621.7	592.1	NA	NA	609.1
Run 2	105.7	1.41	1.35	34.6%	588.6	599.5	589.4	NA	NA	594.5
Run 3	105.3	1.40	1.34	34.2%	610.8	623.3	613.5	NA	NA	618.4
Run 4	105.0	1.40	1.34	33.8%	643.5	681.3	623.7	NA	NA	652.5
Average	105.2	1.40	1.34	34.0%	651.3	671.5	625.2	NA	NA	648.4
										621.8

	Force (lb _f)				Average	Shear Stress (kilodynes/cm ²)					
	Zone 1	Zone 2	Zone 3	Zone 4	Zone 5	Zone 1	Zone 2	Zone 3	Zone 4	Zone 5	Average
Zone 1	NA	NA	NA	NA	NA	NA	NA	NA	NA	NA	NA
Zone 2	NA	NA	NA	NA	NA	NA	NA	NA	NA	NA	NA
Zone 3	NA	NA	NA	NA	NA	NA	NA	NA	NA	NA	NA
Zone 4	NA	NA	NA	NA	NA	NA	NA	NA	NA	NA	NA
Zone 5	NA	NA	NA	NA	NA	NA	NA	NA	NA	NA	NA
					NA						NA

ID # = S36
 Speed = 4 in/min
 S Rate = 1072 s⁻¹
 Temp = 270 °C

	Extrudate Swell (mm)				Viscosity (Pa*s)				
	Screen	Actual	Ratio	%	Zone 1	Zone 2	Zone 3	Zone 4	Zone 5
Run 1	107.3	1.43	1.37	36.8%	203.9	296.7	318.6	316.9	310.7
Run 2	107.0	1.43	1.36	36.3%	292.0	290.6	306.5	293.1	291.9
Run 3	106.7	1.42	1.36	35.9%	280.2	319.4	326.5	328.2	324.7
Run 4	107.0	1.43	1.36	36.3%	317.7	393.5	355.4	359.4	357.4
Average	107.0	1.43	1.36	36.3%	270.3	314.3	343.6	386.0	348.0
									335.2

	Force (lb _f)				Average	Shear Stress (kilodynes/cm ²)				
	Zone 1	Zone 2	Zone 3	Zone 4	Zone 5	Zone 1	Zone 2	Zone 3	Zone 4	Zone 5
Zone 1	209.7	305.1	327.6	325.8	319.5	219.2	319.0	342.5	340.7	334.1
Zone 2	300.2	298.8	315.1	301.4	300.1	312.9	312.4	329.5	315.1	313.5
Zone 3	288.1	328.4	335.7	337.5	333.9	301.2	343.4	351.0	352.9	349.1
Zone 4	326.7	404.6	365.4	369.5	367.5	341.6	423.1	382.1	386.4	384.3
Zone 5	277.9	323.2	353.3	396.9	357.8	290.6	337.9	369.4	415.0	374.1
					344.7					360.4

ID # = S31
 Speed = 10 in/min
 S Rate = 2681 s⁻¹
 Temp = 270 °C

	Extrudate Swell (mm)				Viscosity (Pa*s)				
	Screen	Actual	Ratio	%	Zone 1	Zone 2	Zone 3	Zone 4	Zone 5
Run 1	109.7	1.46	1.40	39.7%	190.9	196.9	108.4	171.2	193.9
Run 2	110.7	1.48	1.41	41.0%	193.1	191.4	189.0	184.4	191.2
Run 3	108.7	1.45	1.38	38.5%	207.4	196.6	190.6	186.4	193.6
Run 4	109.3	1.46	1.39	39.3%	230.8	210.6	196.6	201.7	203.0
Average	109.6	1.46	1.40	39.6%	244.8	211.0	195.6	199.2	201.9
									192.9

	Force (lb _f)				Average	Shear Stress (kilodynes/cm ²)				
	Zone 1	Zone 2	Zone 3	Zone 4	Zone 5	Zone 1	Zone 2	Zone 3	Zone 4	Zone 5
Zone 1	440.8	506.2	2.8	440.2	440.5	513.2	529.3	29.2	460.3	521.3
Zone 2	497.8	492.0	485.9	474	487.4	520.5	514.5	508.1	495.6	509.7
Zone 3	533.1	505.4	484.8	478.9	500.6	557.4	528.5	512.2	500.8	524.7
Zone 4	593.2	541.4	505.5	518.5	521.8	620.3	566.1	528.6	424.2	534.8
Zone 5	629.3	542.5	502.8	512.2	519.2	658.0	567.3	525.7	535.6	542.9
					507.2					526.7

ID # = S32
 Speed = 20 in/min
 S Rate = 5362 s⁻¹
 Temp = 270 °C

	Extrudate Swell (mm)				Viscosity (Pa·s)				
	Screen	Actual	Ratio	%	Zone 1	Zone 2	Zone 3	Zone 4	Zone 5
Run 1	114.3	1.52	1.46	45.7%	643.9	63.0	36.9	45.3	41.1
Run 2	115.0	1.53	1.47	46.5%	123.9	134.2	124.4	127.4	125.2
Run 3	114.5	1.53	1.46	45.9%	125.7	133.8	123.0	129.8	126.2
Run 4	114.0	1.52	1.45	45.2%	131.7	144.0	130.7	136.2	132.9
Average	114.5	1.53	1.46	45.8%	133.7	139.8	136.1	134.6	136.1
									130.1

	Force (lb _f)				Average	Shear Stress (kilodynes/cm ²)				
	Zone 1	Zone 2	Zone 3	Zone 4	Zone 5	Zone 1	Zone 2	Zone 3	Zone 4	Zone 5
Zone 1	33.1	323.9	1.9	233.1	278.5	346.1	338.7	19.8	243.7	342.4
Zone 2	637.3	689.9	639.8	655.0	644.0	666.4	721.4	669.0	684.9	673.4
Zone 3	646.2	688.2	632.7	667.4	648.8	675.7	719.6	661.6	697.9	678.4
Zone 4	677.1	740.6	672.2	700.1	683.1	708.0	774.4	702.9	732.1	714.3
Zone 5	687.3	718.8	699.7	692.0	699.5	718.7	751.6	731.7	723.6	731.4
					668.8					688.7

ID # = S33
 Speed = 30 in/min
 S Rate = 8043 s⁻¹
 Temp = 270 °C

	Extrudate Swell (mm)				Viscosity (Pa·s)				
	Screen	Actual	Ratio	%	Zone 1	Zone 2	Zone 3	Zone 4	Zone 5
Run 1	116.5	1.55	1.48	48.4%	69.2	137.5	79.4	67.4	72.0
Run 2	117.0	1.56	1.49	49.1%	84.0	86.1	87.5	91.1	88.2
Run 3	116.7	1.56	1.49	48.6%	89.4	85.4	87.0	88.1	88.2
Run 4	116.7	1.56	1.49	48.6%	94.0	87.8	91.9	92.7	91.6
Average	116.7	1.56	1.49	48.7%	96.1	87.0	90.8	87.2	88.3
									88.2

	Force (lb _f)				Average	Shear Stress (kilodynes/cm ²)				
	Zone 1	Zone 2	Zone 3	Zone 4	Zone 5	Zone 1	Zone 2	Zone 3	Zone 4	Zone 5
Zone 1	534.1	10.3	612.4	520	555.5	558.5	107.7	640.4	593.7	597.5
Zone 2	686.5	664.5	675.4	703.1	682.4	717.9	694.8	706.2	735.2	713.5
Zone 3	689.3	659.0	670.8	679.4	674.6	720.8	689.1	701.4	710.4	705.4
Zone 4	731.2	677.4	708.6	715.3	708.1	764.6	708.3	741.0	748.0	740.5
Zone 5	741.0	671.4	700.8	673	681.7	774.8	702.1	732.8	703.7	712.9
					679.6					710.6

ID # = S34
 Speed = 40 in/min
 S Rate = 10672 s⁻¹
 Temp = 270 °C

	Extrudate Swell (mm)			
	Screen	Actual	Ratio	%
Run 1	117.3	1.56	1.49	49.4%
Run 2	118.0	1.57	1.50	50.3%
Run 3	118.0	1.57	1.50	50.3%
Run 4	117.7	1.57	1.50	49.9%
Average	117.7	1.57	1.50	50.0%

	Viscosity (Pa•s)				
	Zone 1	Zone 2	Zone 3	Zone 4	
Zone 1	56.9	24.3	306.4	44.7	50.8
Zone 2	157.2	55.9	71.0	74.9	73.0
Zone 3	64.2	62.5	69.7	73.3	67.4
Zone 4	75.5	75.5	72.3	78.7	75.5
Zone 5	74.3	71.5	74.7	78.4	74.7
					74.4

	Force (lb _f)				Average
	Zone 1	Zone 2	Zone 3	Zone 4	
Zone 1	585.2	2.5	31.5	4.6	3.6
Zone 2	588.9	575.3	730.1	770.8	666.3
Zone 3	660.7	643.4	716.8	754.1	693.8
Zone 4	777.0	776.2	743.4	809.7	776.6
Zone 5	763.9	735.2	768.9	807	768.8
					746.4

	Shear Stress (kilodynes/cm ²)				
	Zone 1	Zone 2	Zone 3	Zone 4	
Zone 1	611.9	261.0	329.4	48.1	312.6
Zone 2	615.8	601.6	763.4	806.0	696.7
Zone 3	690.9	672.8	749.5	788.5	725.4
Zone 4	812.5	811.7	777.4	846.7	812.1
Zone 5	798.8	768.8	804.0	843.9	803.9
					759.5

ID # = S35
 Speed = 50 in/min
 S Rate = 13340 s⁻¹
 Temp = 270 °C

	Extrudate Swell (mm)			
	Screen	Actual	Ratio	%
Run 1	118.7	1.58	1.51	51.2%
Run 2	119.0	1.59	1.52	51.6%
Run 3	119.0	1.59	1.52	51.6%
Run 4	118.5	1.58	1.51	51.0%
Average	118.8	1.58	1.51	51.4%

	Viscosity (Pa•s)				
	Zone 1	Zone 2	Zone 3	Zone 4	
Zone 1	12.4	11.8	14.7	24.9	13.0
Zone 2	54.1	55.1	53.9	58.3	54.4
Zone 3	54.1	55.5	53.7	54.8	54.5
Zone 4	55.0	60.2	55.8	56.3	55.7
Zone 5	56.9	56.9	57.4	61.3	57.1
					54.9

	Force (lb _f)				Average
	Zone 1	Zone 2	Zone 3	Zone 4	
Zone 1	1.6	151.9	1.9	3.2	2.2
Zone 2	695.4	708.6	693.7	749.3	699.2
Zone 3	696.3	714.3	690.7	705.3	701.7
Zone 4	707.4	774.6	717.6	723.5	716.2
Zone 5	732.1	732.1	738.5	788.1	734.2
					705.7

	Shear Stress (kilodynes/cm ²)				
	Zone 1	Zone 2	Zone 3	Zone 4	
Zone 1	16.7	158.8	19.8	33.4	23.3
Zone 2	767.2	771.0	775.4	783.5	771.2
Zone 3	768.1	776.9	772.2	767.5	771.2
Zone 4	769.7	810.0	770.4	776.5	772.2
Zone 5	775.5	775.5	772.2	824.1	774.4
					772.2

APPENDIX B

EXPERIMENTAL CAPILLARY DATA FOR REX15/F PET

ID # = 118
 Speed = 0.5 in/min
 S Rate = 134 s⁻¹
 Temp = 290 °C

	Extrudate Swell (mm)				Viscosity (Pa*s)				
	Screen	Actual	Ratio	%	Zone 1	Zone 2	Zone 3	Zone 4	Zone 5
Run 1	165.3	2.20	2.11	110.7%	148.6	277.8	264.5	127.6	204.6
Run 2	167.3	2.23	2.13	113.1%	191.4	238.9	382.8	354.0	325.2
Run 3	165.3	2.20	2.11	110.5%	298.0	292.5	352.5	352.5	323.9
Run 4	166.2	2.22	2.12	111.8%	385.2	344.7	409.3	445.1	413.2
Average	166.0	2.21	2.12	111.5%	336.1	409.3	441.2	457.5	436.0
									374.6

	Force (lb _f)				Average	Shear Stress (kilodynes/cm ²)				
	Zone 1	Zone 2	Zone 3	Zone 4	Zone 5	Zone 1	Zone 2	Zone 3	Zone 4	Zone 5
Zone 1	19.1	35.7	34.0	16.4	26.3	199.7	373.3	355.5	171.4	275.0
Zone 2	24.6	30.7	39.2	45.5	38.5	257.2	321.0	514.5	475.8	437.1
Zone 3	38.3	37.6	45.3	45.3	41.6	400.5	393.1	473.7	473.7	435.3
Zone 4	49.5	44.3	52.6	57.2	53.1	517.6	463.2	550.0	598.1	555.2
Zone 5	43.2	52.6	56.7	58.8	56.0	451.7	550.0	592.9	614.8	585.9
					50.3					503.4

ID # = 117
 Speed = 1 in/min
 S Rate = 268 s⁻¹
 Temp = 290 °C

	Extrudate Swell (mm)				Viscosity (Pa*s)				
	Screen	Actual	Ratio	%	Zone 1	Zone 2	Zone 3	Zone 4	Zone 5
Run 1	215.7	2.88	2.75	174.8%	188.3	335.3	333.0	-	334.2
Run 2	211.0	2.81	2.69	168.8%	238.5	367.6	299.2	-	333.4
Run 3	214.7	2.86	2.74	173.5%	328.7	340.4	363.8	-	344.3
Run 4	214.3	2.86	2.73	173.1%	367.6	380.1	373.1	-	370.4
Average	213.9	2.85	2.73	172.6%	381.3	378.1	387.5	-	382.3
									357.6

	Force (lb _f)				Average	Shear Stress (kilodynes/cm ²)				
	Zone 1	Zone 2	Zone 3	Zone 4	Zone 5	Zone 1	Zone 2	Zone 3	Zone 4	Zone 5
Zone 1	46.4	86.2	85.6	-	85.9	506.1	901.4	895.1	-	898.3
Zone 2	61.3	94.5	76.9	-	69.1	641.0	988.2	804.1	-	896.2
Zone 3	84.5	87.5	93.5	-	88.5	883.6	915.0	977.7	-	925.4
Zone 4	94.5	97.7	95.9	-	95.2	988.2	1021	1002	-	995.1
Zone 5	98.0	97.2	99.6	-	98.3	1024	1016	1041	-	1027
					92.0					960.9

ID # = 111
 Speed = 4 in/min
 S Rate = 1072 s⁻¹
 Temp = 290 °C

	Extrudate Swell (mm)			
	Screen	Actual	Ratio	%
Run 1	229.3	3.06	2.92	192.2%
Run 2	223.3	2.98	2.85	184.6%
Run 3	228.5	3.05	2.91	191.1%
Run 4	225.3	3.00	2.87	187.0%
Average	226.6	3.02	2.89	188.7%

	Viscosity (Pa*s)				
	Zone 1	709.9	92.1	86.0	192.0
Zone 2	197.0	230.9	221.5	195.4	211.2
Zone 3	200.0	229.6	226.9	197.6	213.5
Zone 4	222.3	278.6	254.3	225.8	234.1
Zone 5	212.6	252.8	255.0	222.1	235.6
					223.6

	Force (lb _f)				Average
	Zone 1	215.8	94.7	88.5	197.4
Zone 2	202.6	237.4	227.8	200.9	217.2
Zone 3	205.7	236.1	233.3	203.2	219.6
Zone 4	228.6	286.5	261.5	232.2	240.8
Zone 5	218.6	259.9	262.2	228.4	242.3
					229.9

	Shear Stress (kilodynes/cm ²)				
	Zone 1	225.6	990.3	925.4	206.4
Zone 2	211.8	248.2	238.2	210.0	227.1
Zone 3	215.1	246.8	243.9	212.4	229.6
Zone 4	239.0	299.6	273.4	242.8	251.7
Zone 5	228.5	271.7	274.1	238.8	253.3
					240.4

ID # = 112
 Speed = 10 in/min
 S Rate = 2681 s⁻¹
 Temp = 290 °C

	Extrudate Swell (mm)			
	Screen	Actual	Ratio	%
Run 1	224.3	2.99	2.86	185.7%
Run 2	221.3	2.95	2.82	182.0%
Run 3	223.0	2.97	2.84	184.1%
Run 4	225.0	3.00	2.87	186.7%
Average	223.4	2.98	2.85	184.6%

	Viscosity (Pa*s)				
	Zone 1	571.9	55.5	44.2	77.6
Zone 2	133.0	146.6	142.3	144.6	144.5
Zone 3	142.6	141.6	133.6	142.1	142.1
Zone 4	178.9	163.8	156.9	176.5	173.1
Zone 5	153.2	168.0	147.2	170.7	159.8
					148.8

	Force (lb _f)				Average
	Zone 1	14.7	142.8	113.6	199.5
Zone 2	342.0	376.8	365.9	371.7	371.5
Zone 3	366.6	364.0	343.5	365.4	365.3
Zone 4	459.9	421.2	403.4	453.7	444.9
Zone 5	393.8	431.9	378.5	438.9	421.5
					400.8

	Shear Stress (kilodynes/cm ²)				
	Zone 1	153.7	142.8	118.7	208.6
Zone 2	357.6	376.8	382.6	388.7	382.7
Zone 3	383.3	364.0	359.2	382.1	372.2
Zone 4	480.9	421.2	421.8	474.4	449.6
Zone 5	411.8	431.9	395.8	458.9	434.2
					409.7

ID # = 113
 Speed = 20 in/min
 S Rate = 5362 s⁻¹
 Temp = 290 °C

	Extrudate Swell (mm)				Viscosity (Pa•s)				
	Screen	Actual	Ratio	%	Zone 1	Zone 2	Zone 3	Zone 4	Zone 5
Run 1	208.3	2.78	2.65	165.4%	30.1	34.6	511.6	972.7	32.4
Run 2	206.5	2.75	2.63	163.1%	110.1	104.3	97.7	100.9	105.1
Run 3	221.0	2.95	2.82	181.6%	112.4	108.1	94.8	99.6	103.7
Run 4	213.3	2.84	2.72	171.8%	120.1	99.3	105.5	101.8	102.2
Average	212.3	2.83	2.70	170.5%	112.8	127.5	113.3	114.8	113.6
									106.2

	Force (lb _f)				Average	Shear Stress (kilodynes/cm ²)				
	Zone 1	Zone 2	Zone 3	Zone 4	Zone 5	Zone 1	Zone 2	Zone 3	Zone 4	Zone 5
Zone 1	154.8	178.1	26.3	37.7	166.5	161.8	186.2	275.0	394.2	254.3
Zone 2	566.0	536.6	502.4	508.5	515.8	591.8	561.1	525.3	531.7	552.5
Zone 3	577.8	556.1	487.5	514.0	519.2	604.2	581.5	509.7	537.5	558.2
Zone 4	617.7	510.5	542.6	636.7	576.9	645.9	533.8	567.4	665.8	603.2
Zone 5	579.9	655.4	582.8	448.1	581.4	606.4	685.3	609.4	468.5	592.4
					548.3					576.6

ID # = 114
 Speed = 30 in/min
 S Rate = 8043 s⁻¹
 Temp = 290 °C

	Extrudate Swell (mm)				Viscosity (Pa•s)				
	Screen	Actual	Ratio	%	Zone 1	Zone 2	Zone 3	Zone 4	Zone 5
Run 1	217.5	2.90	2.77	177.1%	158.2	12.1	59.6	359.2	147.3
Run 2	207.5	2.77	2.64	164.4%	70.2	90.3	90.2	72.4	80.8
Run 3	211.5	2.82	2.69	169.5%	86.2	89.3	98.4	72.9	91.3
Run 4	211.5	2.82	2.69	169.5%	92.0	98.7	96.3	77.9	95.7
Average	212.0	2.83	2.70	170.1%	65.6	85.4	94.8	73.9	84.7
									88.1

	Force (lb _f)				Average	Shear Stress (kilodynes/cm ²)				
	Zone 1	Zone 2	Zone 3	Zone 4	Zone 5	Zone 1	Zone 2	Zone 3	Zone 4	Zone 5
Zone 1	12.2	93.4	459.9	27.7	148.3	127.5	976.7	480.9	289.6	468.7
Zone 2	541.4	697.0	695.5	558.4	623.1	566.1	728.8	727.3	583.9	651.5
Zone 3	664.9	689.0	759.2	562.3	704.4	695.3	720.5	793.9	588.0	736.6
Zone 4	707.8	761.5	742.9	601.1	737.4	742.2	796.3	776.8	628.5	771.8
Zone 5	505.8	658.9	731.7	569.9	653.5	528.9	689.0	765.1	595.9	683.3
					679.6					710.8

ID # = 115
 Speed = 40 in/min
 S Rate = 10672 s⁻¹
 Temp = 290 °C

	Extrudate Swell (mm)				Viscosity (Pa*s)				
	Screen	Actual	Ratio	%	Zone 1	Zone 2	Zone 3	Zone 4	Zone 5
Run 1	226.0	3.01	2.88	187.9%	33.1	334.6	32.7	11.0	25.6
Run 2	214.5	2.86	2.73	173.3%	62.9	62.7	72.3	56.2	66.0
Run 3	208.5	2.78	2.66	165.7%	58.9	61.9	66.4	56.2	62.4
Run 4	216.0	2.88	2.75	175.2%	73.9	71.7	76.9	66.0	74.2
Average	216.3	2.88	2.76	175.5%	65.7	68.8	67.1	62.8	67.2
									67.4

	Force (lb _f)				Average	Shear Stress (kilodynes/cm ²)				
	Zone 1	Zone 2	Zone 3	Zone 4	Zone 5	Zone 1	Zone 2	Zone 3	Zone 4	Zone 5
Zone 1	340.8	34.4	336.2	113.4	338.5	356.3	359.7	351.5	118.5	355.8
Zone 2	646.7	644.6	744.1	578.1	645.7	676.2	674.0	778.1	604.5	675.1
Zone 3	606.2	636.5	682.9	577.9	641.9	633.9	665.6	714.1	604.3	671.2
Zone 4	760.7	737.1	791.5	678.6	763.1	765.4	770.8	827.7	709.6	788.0
Zone 5	676.0	707.9	690.7	646.0	691.5	706.9	740.2	722.2	675.5	723.1
					685.5					714.3

ID # = 116
 Speed = 50 in/min
 S Rate = 13340 s⁻¹
 Temp = 290 °C

	Extrudate Swell (mm)				Viscosity (Pa*s)				
	Screen	Actual	Ratio	%	Zone 1	Zone 2	Zone 3	Zone 4	Zone 5
Run 1	225.0	3.00	2.87	186.7%	14.7	10.4	29.3	13.0	12.7
Run 2	222.0	2.96	2.83	182.9%	48.2	48.9	48.3	43.6	48.5
Run 3	226.7	3.02	2.89	188.8%	46.0	47.5	47.6	48.3	47.4
Run 4	222.5	2.97	2.83	183.5%	51.1	51.4	58.0	51.2	51.2
Average	224.0	2.99	2.85	185.5%	48.2	51.3	48.2	48.8	48.4
									48.9

	Force (lb _f)				Average	Shear Stress (kilodynes/cm ²)				
	Zone 1	Zone 2	Zone 3	Zone 4	Zone 5	Zone 1	Zone 2	Zone 3	Zone 4	Zone 5
Zone 1	189.7	134.0	377.4	168.0	163.9	198.3	140.1	399.6	175.6	171.3
Zone 2	582.1	589.9	582.6	560.9	584.9	608.7	616.8	604.2	586.5	609.9
Zone 3	591.3	611.0	586.8	582.5	592.9	618.3	638.9	613.6	609.1	620.0
Zone 4	657.1	661.4	746.5	658.5	659.0	687.1	691.6	780.6	688.6	689.1
Zone 5	620.6	659.9	620.6	627.4	622.9	648.9	690.0	648.9	656.0	651.3
					614.9					642.6

ID # = 121
 Speed = 4 in/min
 S Rate = 1072 s⁻¹
 Temp = 280 °C

	Extrudate Swell (mm)				Viscosity (Pa*s)				
	Screen	Actual	Ratio	%	Zone 1	Zone 2	Zone 3	Zone 4	Zone 5
Run 1	245.2	3.27	3.12	212.4%	56.9	216.8	244.6	211.7	224.4
Run 2	236.6	3.15	3.01	201.5%	263.1	291.1	263.0	282.9	275.0
Run 3	242.5	3.23	3.09	209.0%	310.3	300.0	294.8	252.0	301.7
Run 4	241.0	3.21	3.07	207.1%	313.6	327.4	341.3	305.2	315.4
Average	241.3	3.22	3.07	207.5%	290.0	322.6	315.4	297.2	311.7
									309.6

	Force (lb _f)				Average	Shear Stress (kilodynes/cm ²)				
	Zone 1	Zone 2	Zone 3	Zone 4	Zone 5	Zone 1	Zone 2	Zone 3	Zone 4	Zone 5
Zone 1	58.5	222.9	251.5	217.7	230.7	611.7	233.0	263.0	227.6	241.2
Zone 2	270.5	299.3	270.4	290.9	282.8	282.8	312.9	282.7	304.2	295.7
Zone 3	319.1	308.5	303.1	259.1	310.2	333.6	322.6	316.9	270.9	324.4
Zone 4	321.4	336.6	350.9	313.9	324.0	336.1	351.9	366.9	328.2	338.7
Zone 5	298.2	331.7	324.3	305.7	320.6	311.8	346.8	339.1	319.6	335.2
					318.3					332.8

ID # = 122
 Speed = 10 in/min
 S Rate = 2681 s⁻¹
 Temp = 280 °C

	Extrudate Swell (mm)				Viscosity (Pa*s)				
	Screen	Actual	Ratio	%	Zone 1	Zone 2	Zone 3	Zone 4	Zone 5
Run 1	226.0	3.01	2.88	187.9%	117.3	36.2	143.6	124.7	128.5
Run 2	222.0	2.96	2.83	182.9%	162.2	165.4	174.4	235.0	167.3
Run 3	222.5	2.97	2.83	183.5%	239.2	163.7	218.8	202.4	220.1
Run 4	227.3	3.03	2.90	189.6%	202.4	190.0	240.6	252.7	231.9
Average	224.5	2.99	2.86	186.0%	221.8	163.2	247.0	257.2	242.0
									231.3

	Force (lb _f)				Average	Shear Stress (kilodynes/cm ²)				
	Zone 1	Zone 2	Zone 3	Zone 4	Zone 5	Zone 1	Zone 2	Zone 3	Zone 4	Zone 5
Zone 1	301.6	93.2	367.1	320.5	329.7	315.3	974.6	385.9	335.1	345.4
Zone 2	417.0	425.2	451.0	604.0	431.1	436.0	444.6	471.6	631.6	450.7
Zone 3	615.0	420.8	562.4	520.2	565.9	643.1	440.0	588.1	543.9	591.7
Zone 4	520.2	488.5	618.4	649.7	596.1	543.9	510.8	646.6	679.4	623.3
Zone 5	570.2	419.6	634.9	661.1	622.1	596.2	438.7	663.9	691.3	650.5
					594.7					621.8

ID # = 123
 Speed = 20 in/min
 S Rate = 5362 s⁻¹
 Temp = 280 °C

	Extrudate Swell (mm)			
	Screen	Actual	Ratio	%
Run 1	218.0	2.91	2.78	177.8%
Run 2	216.3	2.88	2.76	175.6%
Run 3	216.5	2.89	2.76	175.8%
Run 4	215.0	2.87	2.74	173.9%
Average	216.5	2.89	2.76	175.8%

	Viscosity (Pa*s)				
	Zone 1	19.6	74.1	54.2	59.2
Zone 2	124.6	153.7	143.3	125.9	136.9
Zone 3	144.3	134.4	122.3	120.9	130.5
Zone 4	149.0	155.5	146.3	133.4	150.3
Zone 5	155.1	153.8	144.8	127.2	151.2
					142.2

	Force (lb _f)				Average
	Zone 1	100.9	381.1	278.6	304.8
Zone 2	640.7	790.2	736.8	647.4	703.8
Zone 3	741.8	690.9	628.8	621.5	670.8
Zone 4	766.0	799.6	752.2	685.9	772.6
Zone 5	797.6	790.9	744.6	654.1	777.7
					731.2

	Shear Stress (kilodynes/cm ²)				
	Zone 1	105.5	398.5	291.3	318.7
Zone 2	670.0	826.3	770.5	677.0	736.0
Zone 3	775.7	722.5	657.5	649.9	701.4
Zone 4	801.0	836.1	786.6	717.2	807.9
Zone 5	834.0	827.0	778.6	684.0	813.2
					764.6

ID # = 132
 Speed = 0.5 in/min
 S Rate = 134 s⁻¹
 Temp = 270 °C

	Extrudate Swell (mm)			
	Screen	Actual	Ratio	%
Run 1	245.8	3.28	3.13	213.1%
Run 2	248.3	3.31	3.16	216.4%
Run 3	251.5	3.35	3.20	220.4%
Run 4	244.0	3.25	3.11	210.9%
Average	247.4	3.30	3.15	215.2%

	Viscosity (Pa*s)				
	Zone 1	808.5	437.3	669.2	366.5
Zone 2	680.1	718.2	750.1	719.8	717.1
Zone 3	718.2	981.2	795.3	747.0	753.5
Zone 4	753.2	866.8	826.4	828.7	840.6
Zone 5	943.9	1011.8	973.5	986.7	979.0
					822.5

	Force (lb _f)				Average
	Zone 1	103.9	56.2	86.0	47.1
Zone 2	87.4	12.3	96.4	92.5	92.1
Zone 3	92.3	126.1	102.2	96.0	104.2
Zone 4	96.8	111.4	106.2	106.5	105.2
Zone 5	121.3	152.3	125.1	126.8	124.4
					106.5

	Shear Stress (kilodynes/cm ²)				
	Zone 1	108.6	587.7	849.3	992.5
Zone 2	913.9	965.2	100.8	967.3	948.8
Zone 3	965.2	131.8	106.8	100.3	113.0
Zone 4	101.2	116.4	111.0	111.3	110.0
Zone 5	126.8	159.2	130.8	132.6	130.1
					117.7

ID # = 131
 Speed = 1 in/min
 S Rate = 268 s⁻¹
 Temp = 270 °C

Extrudate Swell (mm)					Viscosity (Pa•s)					
	Screen	Actual	Ratio	%						
Run 1	255.0	3.40	3.25	224.9%	Zone 1	457.5	466.5	554.8	484.0	469.3
Run 2	254.7	3.40	3.24	224.5%	Zone 2	906.1	730.3	580.9	637.3	649.5
Run 3	266.5	3.55	3.40	239.6%	Zone 3	1010.1	688.6	572.3	706.9	655.9
Run 4	265.5	3.54	3.38	238.3%	Zone 4	1010.1	844.3	720.2	849.3	804.6
Average	260.4	3.47	3.32	231.8%	Zone 5	763.3	870.0	725.6	780.9	756.6
										716.7

	Force (lb _f)				Average	Shear Stress (kilodynes/cm ²)					
Zone 1	117.6	119.9	142.6	124.4	120.6	Zone 1	122.9	125.3	149.1	130.0	126.1
Zone 2	232.9	187.7	149.3	163.8	166.9	Zone 2	243.5	196.2	156.1	171.2	174.5
Zone 3	260.3	177.0	147.1	181.7	168.6	Zone 3	272.2	185.0	153.8	190.0	176.3
Zone 4	259.7	217.0	185.1	218.3	206.8	Zone 4	271.5	227	194	228.2	216.2
Zone 5	196.2	223.6	186.5	200.7	194.5	Zone 5	205	234	195	209.8	203
					184.2						192.6

APPENDIX C

CORRECTED DATA AND CALCULATION RESULTS

Table C - 1 Rabinowitsch Correction (R_C) for Shell 9506 at 290 °C

$\ln \dot{\gamma}_a$ (s ⁻¹)	$\ln \sigma$ (kdsc)	η_a (Pa·s)	$d \ln \dot{\gamma}_a / d \ln \sigma$	R_C	$\dot{\gamma}_w$ (s ⁻¹)	η (Pa·s)
4.90	5.9	252.8	-	-	134.0	252.8
5.59	6.3	201.1	-	-	268.0	201.1
6.98	5.3	186.0	1.48	1.12	1200.2	166.7
7.89	5.8	119.2	1.98	1.25	3340.2	95.9
8.59	6.1	80.2	2.68	1.42	7607.4	56.8
8.99	6.2	60.6	3.36	1.59	12788.8	36.9
9.28	6.2	45.3	4.09	1.77	18919.2	25.8
9.50	6.3	38.6	4.94	1.98	26475.9	19.7

Table C - 2 Rabinowitsch Correction (R_C) for Shell 9506 at 280 °C

$\ln \dot{\gamma}_a$ (s ⁻¹)	$\ln \sigma$ (kdsc)	η_a (Pa·s)	$d \ln \dot{\gamma}_a / d \ln \sigma$	R_C	$\dot{\gamma}_w$ (s ⁻¹)	η (Pa·s)
4.90	6.4	451.2	-	-	134.0	451.2
5.59	NA	415.2	-	-	268.0	415.2
6.98	5.6	251.4	1.52	1.13	1210.3	223.4
7.89	5.9	141.5	1.94	1.24	3312.1	104.9
8.59	6.4	105.2	2.47	1.37	7326.0	78.4
8.99	6.4	75.6	2.93	1.48	11917.2	51.1
9.28	6.4	56.7	3.37	1.59	16985.8	36.0
9.50	6.4	44.3	3.82	1.70	22742.1	26.2

Table C - 3 Rabinowitsch Correction (R_C) for Shell 9506 at 270 °C

$\ln \dot{\gamma}_a$ (s ⁻¹)	$\ln \sigma$ (kdsc)	η_a (Pa·s)	$d \ln \dot{\gamma}_a / d \ln \sigma$	R_C	$\dot{\gamma}_w$ (s ⁻¹)	η (Pa·s)
4.90	NA	NA	-	-	134.0	NA
5.59	NA	621.8	-	-	268.0	621.8
6.98	5.9	335.2	1.64	1.16	1242.6	290.0
7.89	6.3	192.9	2.16	1.29	3460.0	152.2
8.59	6.5	130.1	2.86	1.46	7849.4	87.7
8.99	6.6	88.2	3.51	1.63	13099.8	54.2
9.28	6.6	74.4	4.19	1.80	19181.7	39.6
9.50	6.6	54.9	4.94	1.98	26470.9	29.2

Table C - 4 R_C Curve Equations for Shell

T = 290 °C y=-0.0974x ² + 1.9828x - 3.7959
T = 280 °C y=-0.0798x ² + 1.6707x - 2.2145
T = 270 °C y=-0.0865x ² + 1.7313x - 1.9846

Table C - 5 Corrected Data for Shell PET 9506

T (°C)	$\dot{\gamma}_w$ (s ⁻¹)	σ (kdsc)	η (Pa·s)	Ratio	E.S. %	(°C)	rad/s	Pa	Pa	Pa·s	g·cm
						Temp	Freq	G'	G''	η^*	Torque
290	134	378.0	252.8	1.17	16.8%	290	0.100	1.047	96.99	970.0	3.017
290	268	540.5	201.1	1.21	20.9%	290	0.2154	2.294	198.6	922.0	6.177
290	1200	200.0	166.7	1.29	29.2%	290	0.4642	5.493	422.1	909.4	13.12
290	3340	320.4	95.9	1.33	32.7%	290	1.00	18.08	900.2	900.4	27.99
290	7607	431.9	56.8	1.40	39.7%	290	2.154	62.29	1918	890.7	59.66
290	12789	471.9	36.9	1.42	41.5%	290	4.642	21.89	4058	875.7	126.3
290	18919	487.3	25.8	1.43	42.7%	290	10.00	72.90	8443	847.5	263.3
290	26476	522.6	19.7	1.43	42.9%	290	21.54	219.6	16730	783.3	523.3
280	134	599.1	451.2	1.24	23.8%	290	46.4	571.5	29580	649.1	924.0
280	268	NA	415.2	1.29	28.7%	290	100.0	178.4	35530	397.6	1155
280	1210	270.3	223.4	1.33	32.7%	280	0.100	4.555	170.0	1701	4.224
280	3312	347.5	104.9	1.36	36.2%	280	0.2154	5.010	322.2	1496	8.005
280	7326	574.1	78.4	1.42	42.1%	280	0.4642	15.61	666.0	1435	16.54
280	11917	608.6	51.1	1.46	45.9%	280	1.00	44.00	1397	1397	34.70
280	16986	611.7	36.0	1.47	47.0%	280	2.154	138.2	2938	1365	73.05
280	22742	595.0	26.2	1.47	47.3%	280	4.642	448.2	6119	1322	152.4
270	134	NA	NA	NA	NA	280	10.00	1395	12460	1254	311.3
270	268	NA	621.8	1.34	34.0%	280	21.54	3990	24160	1137	606.2
270	1243	360.4	290.0	1.36	36.3%	280	46.410	10140	42510	941.7	1070
270	3460	526.7	152.2	1.40	39.6%	280	100.00	20190	59510	628.4	1466
270	7849	688.7	87.7	1.46	45.8%						
270	13100	710.6	54.2	1.49	48.7%						
270	19182	759.5	39.6	1.50	50.0%						
270	26471	772.2	29.2	1.51	51.4%						

Table C - 6 Corrected Data for Sinco B PET

T (°C)	$\dot{\gamma}_w$ (s ⁻¹)	σ (kdsc)	η (Pa·s)	Ratio	E.S. %	(°C)	rad/s	Pa	Pa	Pa·s	g·cm
						Temp	Freq	G'	G''	η^*	Torque
290	134	503.4	374.6	2.12	112%	290	0.100	19.74	321.4	3220	8.013
290	268	960.9	357.6	2.73	173%	290	0.2154	62.22	563.3	2631	14.1
290	1247	240.4	192.8	2.89	189%	290	0.4642	198.4	1066	2336	26.97
290	3249	409.7	126.1	2.85	185%	290	1.00	536.0	1954	2026	50.40
290	6738	576.6	85.6	2.70	170%	290	2.154	1232	3433	1693	90.71
290	10353	710.8	68.7	2.70	170%	290	4.642	2513	5767	1355	156.3
290	13988	714.3	51.1	2.76	176%	290	10.00	4670	9261	1037	257.4
290	17754	642.6	36.2	2.85	185%	290	21.54	7927	14060	749.3	399.3
280	134	786.8	594.6	2.83	183%	290	46.410	12620	20390	516.7	585.7
280	310.2	160.9	518.6	2.88	188%	290	100.00	18390	27130	327.7	761.4
280	1298	332.8	256.4	3.07	207%	280	0.100	51.71	443.9	4469	8.329
280	3364	621.8	184.9	2.86	186%	280	0.2154	160.9	849.7	4014	16.12
280	6937	764.6	110.2	2.76	176%	280	0.4642	452.3	1579	3540	30.61
270	134	117.7	822.5	3.15	215%	280	1.00	1054	2748	2943	54.81
270	268	192.6	716.7	3.32	232%	280	2.154	2159	4606	2361	94.7
						280	4.642	4048	7462	1829	157.9
						280	10.00	7129	11740	1374	255
						280	21.54	11920	17940	999.6	398.3
						280	46.410	19080	26660	706.4	598.2
						280	100.00	28950	37620	474.7	823.5

Table C - 7 Rabinowitsch Correction (R_C) for Sinco B at 290 °C

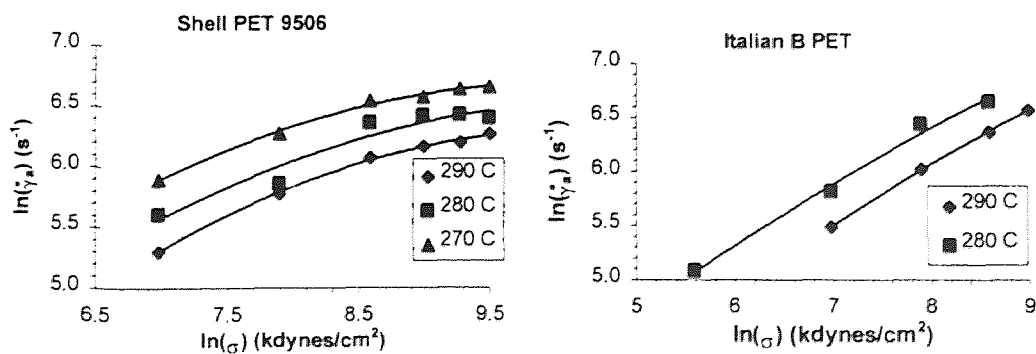
$\ln \dot{\gamma}_a (s^{-1})$	$\ln \sigma (kdsc)$	$\eta_a (Pa \cdot s)$	$d \ln \dot{\gamma}_a / d \ln \sigma$	R_C	$\dot{\gamma}_w (s^{-1})$	$\eta (Pa \cdot s)$
4.90	6.2	374.6	-	-	134.0	374.6
5.59	6.9	357.6	-	-	268.0	357.6
6.98	5.5	223.6	1.65	1.16	1247.1	192.8
7.89	6.0	148.8	1.85	1.21	3248.7	126.1
8.59	6.4	106.2	2.03	1.26	6738.0	85.6
8.99	6.6	88.1	2.15	1.29	10352.6	68.7
9.28	6.6	67.4	2.24	1.31	13988.2	51.1
9.50	6.5	48.9	2.32	1.33	17753.6	36.2

Table C - 8 Rabinowitsch Correction (R_C) for Sinco B at 280 °C

$\ln \dot{\gamma}_a (s^{-1})$	$\ln \sigma (kdsc)$	$\eta_a (Pa \cdot s)$	$d \ln \dot{\gamma}_a / d \ln \sigma$	R_C	$\dot{\gamma}_w (s^{-1})$	$\eta (Pa \cdot s)$
4.90	6.7	594.6	-	-	134.0	594.6
5.59	5.1	593.6	1.63	1.16	310.2	518.6
6.98	5.8	309.6	1.84	1.21	1298.0	256.4
7.89	6.4	231.3	2.02	1.25	3363.8	184.9
8.59	6.6	142.2	2.18	1.29	6937.4	110.2

Table C - 9 R_C Curve Equations for Sinco B

$T = 290 \text{ C}$ $y = -0.0346x^2 + 1.0877x - 0.4193$
$T = 280 \text{ C}$ $y = -0.0257x^2 + 0.9011x + 0.831$

**Figure C - 1** Rabinowitsch Correction Curves for Shell 9506 and Sinco B

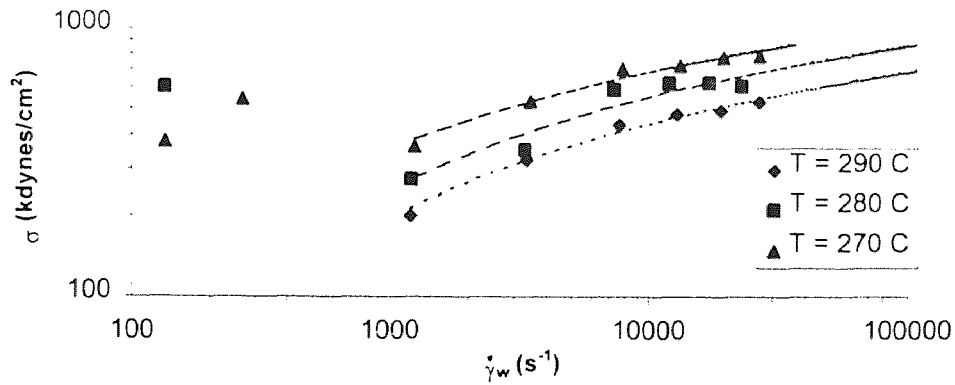


Figure C - 2 Corrected Shear Rate vs. Shear Stress for Shell 9506 PET

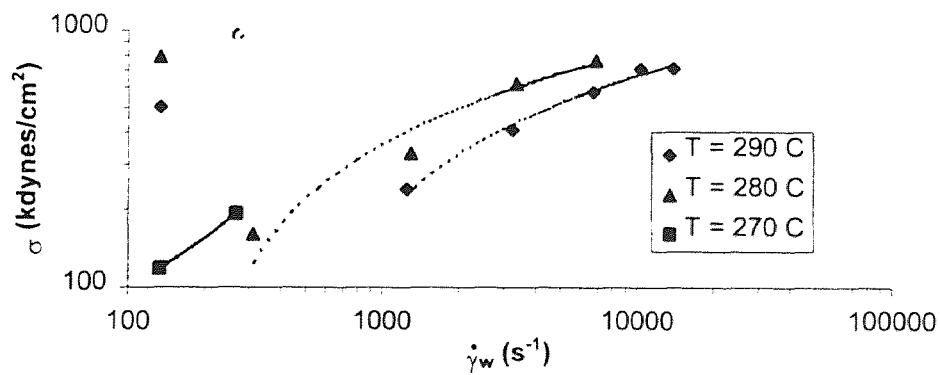


Figure C - 3 Corrected Shear Rate vs. Shear Stress for Sinco B PET

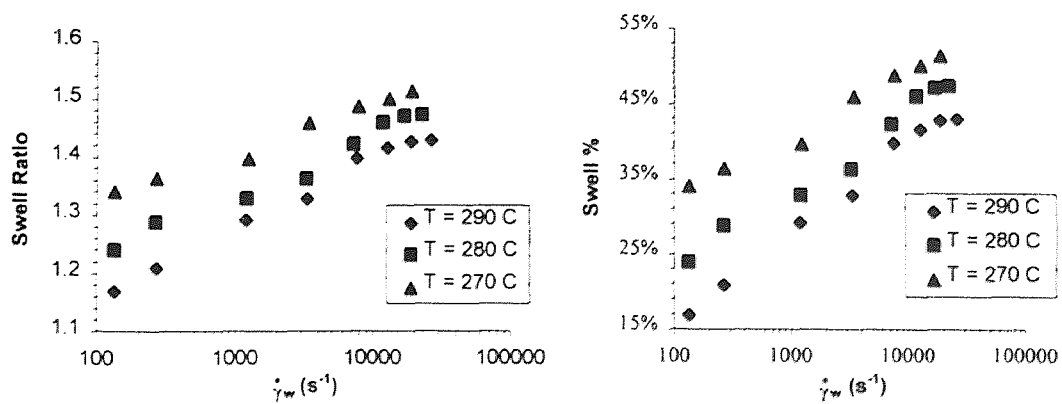


Figure C - 4 Swell ratio and Swell % vs. Shear Rate for Shell 9506

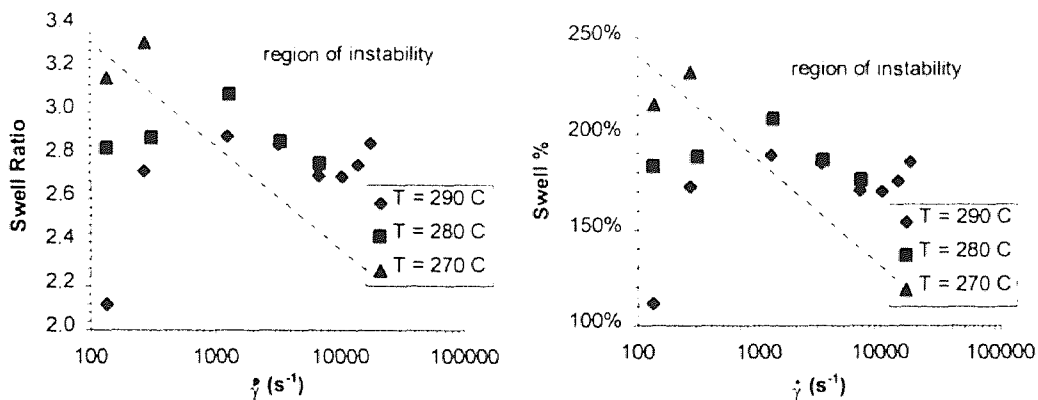


Figure C - 5 Swell Ratio and Swell % vs. Shear Rate for Sinco B

Table C - 10 Activation Energy Dependence on Shear Rate for Shell 9506

a) Viscosity

Average $\dot{\gamma}_w$	E_1 / R_g	E_1 (kJ/mol)
134.0	7831.2	65.1
268.0	7481.3	62.2
1217.7	2976.9	24.7
3370.8	2421.6	20.1
7594.3	2196.9	18.3
12601.9	2011.3	16.7
18362.3	2092.6	17.4
25229.7	1818.9	15.1

b) Die Swell

Average $\dot{\gamma}_w$	E_1 / R_g	E_1 (kJ/mol)
134.0	781.4	6.5
268.0	682.5	5.7
1217.7	358.4	3.0
3370.8	337.4	2.8
7594.3	284.2	2.4
12601.9	327.4	2.7
18362.3	330.8	2.8
25229.7	380.8	3.2

Table C - 11 Complex Viscosity Data for Shell 9506

Temperature = 280 °C

rad/s Freq	Pa G'	Pa G''	Pa*s η^*	g*cm Torque
0.100	4.555	170.0	1701	4.224
0.2154	5.010	322.2	1496	8.005
0.4642	15.61	666.0	1435	16.54
1.00	44.00	1397	1397	34.70
2.154	138.2	2938	1365	73.05
4.642	448.2	6119	1322	152.4
10.00	1395	12460	1254	311.3
21.54	3990	24160	1137	606.2
46.410	10140	42510	942	1070
100.00	20190	59510	628	1466

Temperature = 290 °C

rad/s Freq	Pa G'	Pa G''	Pa*s η^*	g*cm Torque
0.100	1.047	96.99	970.0	3.017
0.2154	2.294	198.6	922.0	6.177
0.4642	5.493	422.1	909	13.12
1.00	18.08	900.2	900	27.99
2.154	62.29	1918	891	59.66
4.642	21.89	4058	876	126.3
10.00	72.90	8443	848	263.3
21.54	219.6	16730	783	523.3
46.410	571.5	29580	649	924.0
100.00	178.4	35530	398	1155

Table C - 12 Complex Viscosity Data for Sinco B

Temperature = 280 °C

rad/s Freq	Pa G'	Pa G''	Pa*s η^*	g*cm Torque
0.100	51.71	443.9	4469	8.329
0.2154	160.9	849.7	4014	16.12
0.4642	452.3	1579	3540	30.61
1.00	1054	2748	2943	54.81
2.154	2159	4606	2361	94.7
4.642	4048	7462	1829	157.9
10.00	7129	11740	1374	255
21.54	11920	17940	999.6	398.3
46.410	19080	26660	706.4	598.2
100.00	28950	37620	474.7	823.5

Temperature = 290 °C

rad/s Freq	Pa G'	Pa G''	Pa*s η^*	g*cm Torque
0.100	19.74	321.4	3220	8.013
0.2154	62.22	563.3	2631	14.1
0.4642	198.4	1066	2336	26.97
1.00	536.0	1954	2026	50.40
2.154	1232	3433	1693	90.71
4.642	2513	5767	1355	156.3
10.00	4670	9261	1037	257.4
21.54	7927	14060	749	399.3
46.410	12620	20390	517	585.7
100.00	18390	27130	328	761.4

Table C - 13 R² Values for Shell 9506 Viscosity Fitting

	B.H,	Eyring	Carreau	Cross	Sutterby	Vino.
280 °C	0.9939	0.9886	0.9878	0.9940	0.9915	0.9941
290 °C	0.9902	0.9936	0.9944	0.9894	0.9938	0.9924
Average	0.9921	0.9911	0.9911	0.9917	0.9927	0.9933

Table C - 14 R² Values for Sinco B Viscosity Fitting

	B.H,	Eyring	Carreau	Cross	Sutterby	Vino.
280 °C	0.9902	0.9747	0.9881	0.9985	0.9978	0.9894
290 °C	0.9884	0.9721	0.9831	0.9974	0.9940	0.9923
Average	0.9893	0.9734	0.9856	0.9980	0.9959	0.9909

APPENDIX D

MODELING RESULTS

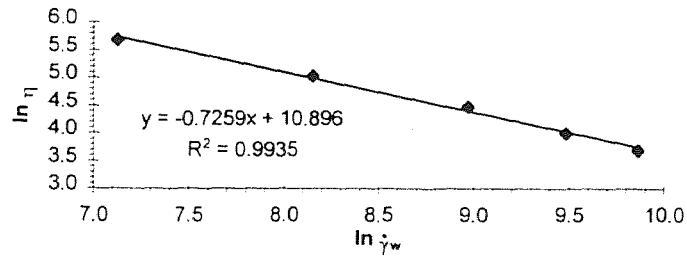


Figure D - 1 Determination of n for Shell 9506 at 270 °C

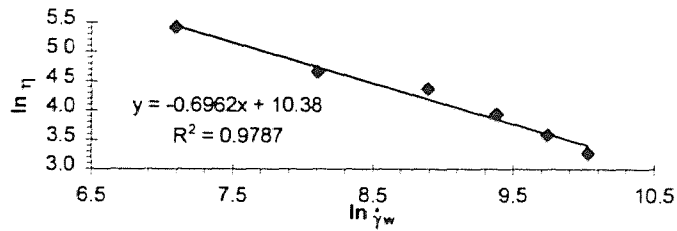


Figure D - 2 Determination of n for Shell 9506 at 280 °C

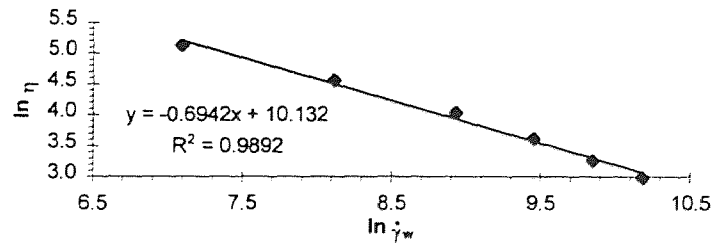


Figure D - 3 Determination of n for Shell 9506 at 290 °C

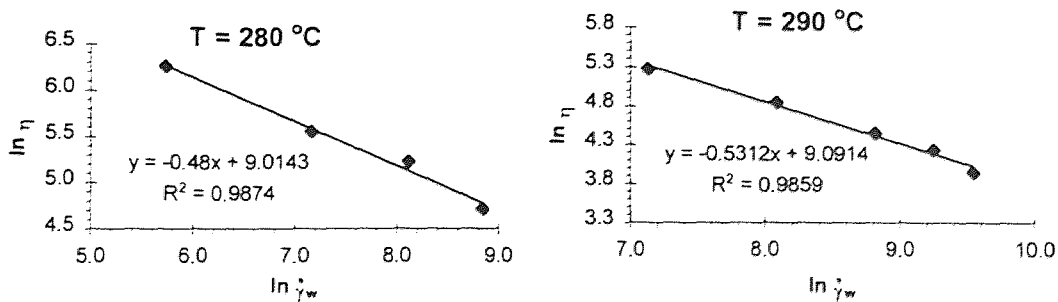


Figure D - 4 Determination of n for Sinco B

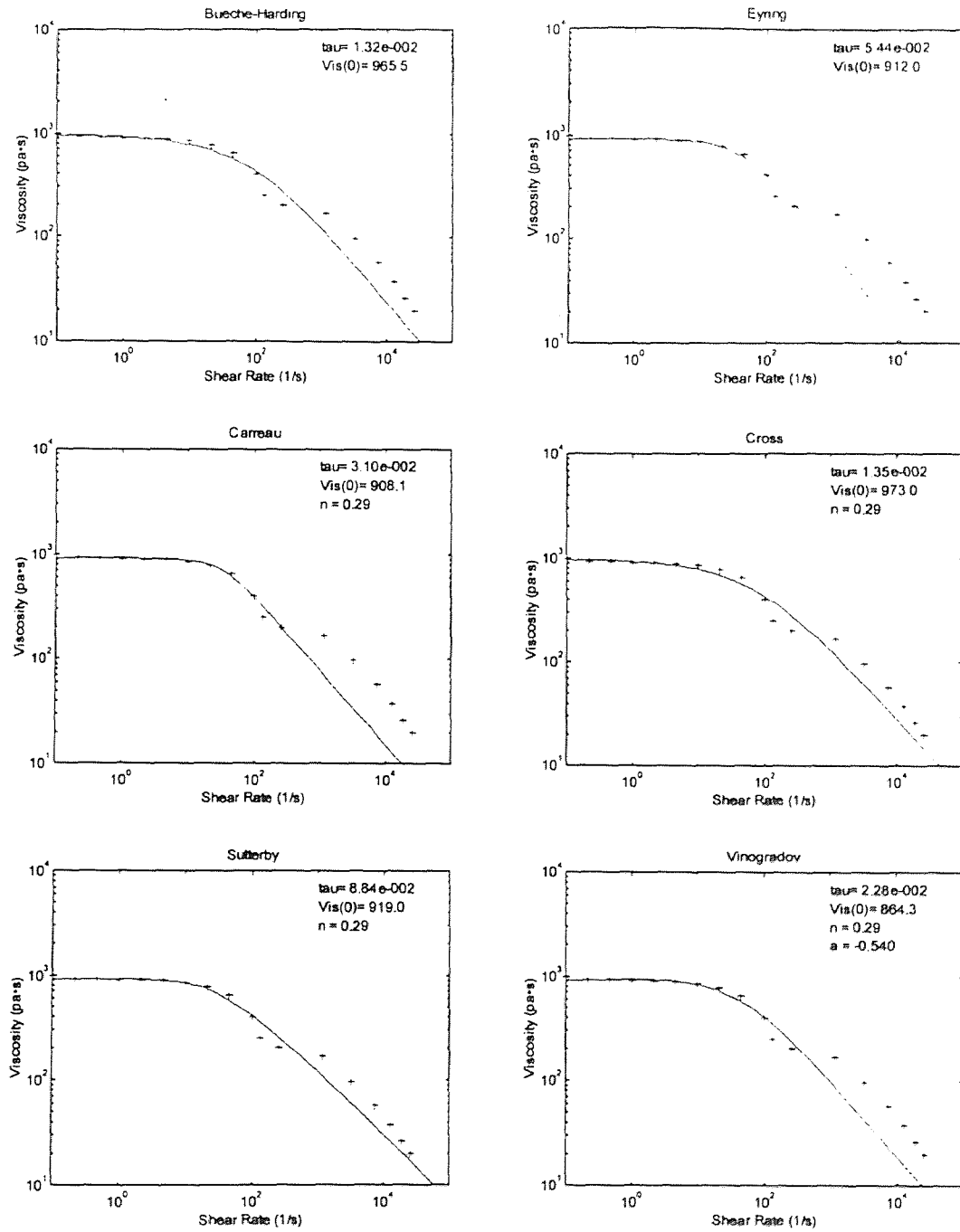


Figure D - 5 Modeling of Shell 9506 at 290 °C

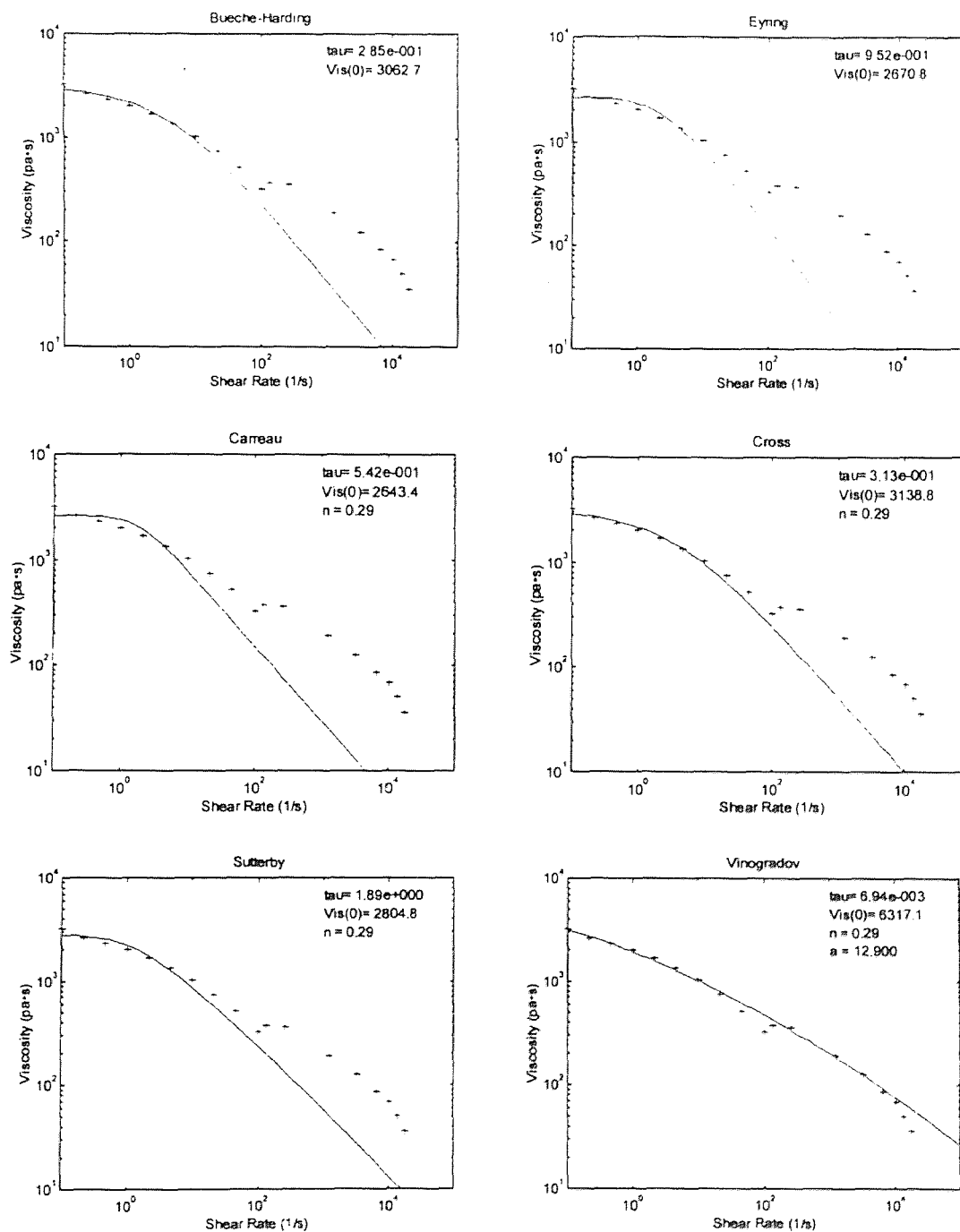


Figure D - 6 Modeling of Sinco B at 290 °C

APPENDIX E

MATLAB MODELING FUNCTIONS AND COMPUTER CODE

Viscosity Modeling Code (visfit.m function):

```
global n f x y

% Experimental Data
Shell290x = [0.100 0.2154 0.4642 1.00 2.154 4.642 10.00 21.54 46.4 100.0 134 268
1200 3340 7607 12788 18919 26475];
Shell290y = [970.0 922.0 909.4 900.4 890.7 875.7 847.5 783.3 649.1 397.6 253 201 167
96 57 37 26 20];
Sinco290x = [0.100 0.2154 0.4642 1.00 2.154 4.642 10.00 21.54 46.410 100.00 134 268
1247 3249 6738 10353 13988 17754];
Sinco290y = [3220 2631 2336 2026 1693 1355 1037 749.3 516.7 327.7 375 358 193 126
86 69 51 36];
Shell280x = [0.100 0.2154 0.4642 1.00 2.154 4.642 10.00 21.54 46.4 100.0 134 268
1210 3312 7326 11917 16986 22742];
Shell280y = [1701 1496 1435 1397 1365 1322 1254 1137 941.7 628.4 451 415 223 105
78 51 36 26];
Sinco280x = [0.100 0.2154 0.4642 1.00 2.154 4.642 10.00 21.54 46.410 100.00 134 310
1298 3364 6937];
Sinco280y = [4469 4014 3540 2943 2361 1829 1374 999.6 706.4 474.7 595 519 256 185
110];

% Initial Variables
n = 0.29;      % Shell 9506 at 290 C Power-Law Index
d = 1;        % 1=Shell 290 C, 2=Shell 280 C, 3=Sinco 290 C, 4=Sinco 280 C
f = 1;        % 1=Bueche-Harding, 2=Eyring, 3=Carreau, 4=Cross, 5=Sutterby,
              % 6=Vinogradov

% Initialize Data Set
if d == 1
x = Shell290x;      % Shear Rate Data
y = Shell290y;      % Viscosity Data
P = 'Shell PET 9506';
T = '290 C';
else if d == 2
    x = Shell280x;      % Shear Rate Data
    y = Shell280y;      % Viscosity Data
    P = 'Shell PET 9506';
```

```

    T = '280 C';
else if d == 3
    x = Sinco290x;      % Shear Rate Data
    y = Sinco290y;      % Viscosity Data
    P = 'Sinco B PET';
    T = '290 C';
else
    x = Sinco280x;      % Shear Rate Data
    y = Sinco280y;      % Viscosity Data
    P = 'Sinco B PET';
    T = '280 C';
end
end
end

% Least-Square Solution
lam = [ .0001 y(1) 0.5 1];
lambda = fmins('fit',lam);
c = lambda(1);          % Characteristic Time Constant
Vo = lambda(2);         % Zero Shear Rate Viscosity
%n = lambda(3);         % Power Law Index (not used)
a = lambda(4);

% Determine fitted line and R2
if f == 1      % Bueche-Harding
    m = 'Bueche-Harding';
    X = logspace(-1,5);
    Y = Vo./(1+(c.*X).^0.75);

    % Coefficient of Determination
    y2 = Vo./(1+(c.*x).^0.75);
    resid = y-y2;
    SSE = sum(resid.^2);
    SSyy = sum((y-mean(y)).^2);
    R2 = sqrt(1-SSE/SSyy)
end

if f == 2      % Eyring
    m = 'Eyring';
    X = logspace(-1,5);
    Y = Vo.*asinh(c.*X)/(c.*X);

    % Coefficient of Determination
    y2 = Vo.*asinh(c.*x)/(c.*x);
    resid = y-y2;

```

```

    SSE = sum(resid.^2);
    SSyy = sum((y-mean(y)).^2);
    R2 = sqrt(1-SSE/SSyy)
end

if f == 3      % Carreau
    m = 'Carreau';
    X = logspace(-1,5);
    Y = Vo.*(1+(c.*X).^2).^((n-1)/2);

    % Coefficient of Determination
    y2 = Vo.*(1+(c.*x).^2).^((n-1)/2);
    resid = y-y2;
    SSE = sum(resid.^2);
    SSyy = sum((y-mean(y)).^2);
    R2 = sqrt(1-SSE/SSyy)
end

if f == 4      % Cross
    m = 'Cross';
    X = logspace(-1,5);
    Y = Vo./(1+(c.*X).^(1-n));

    % Coefficient of Determination
    y2 = Vo./(1+(c.*x).^(1-n));
    resid = y-y2;
    SSE = sum(resid.^2);
    SSyy = sum((y-mean(y)).^2);
    R2 = sqrt(1-SSE/SSyy)
end

if f == 5      % Sutterby
    m = 'Sutterby';
    X = logspace(-1,5);
    Y = Vo.*(asinh(c.*X)/(c.*X)).^(1-n);

    % Coefficient of Determination
    y2 = Vo.*(asinh(c.*x)/(c.*x)).^(1-n);
    resid = y-y2;
    SSE = sum(resid.^2);
    SSyy = sum((y-mean(y)).^2);
    R2 = sqrt(1-SSE/SSyy)
end

if f == 6      % Vinogradov

```



```

m = 'Vinogradov';
X = logspace(-1,5);
Y = Vo./(1+a.*(c.*X).^((1-n)/2)+(c.*X).^((1-n)));

% Coefficient of Determination
y2 = Vo./(1+a.*(c.*x).^((1-n)/2)+(c.*x).^((1-n)));
resid = y-y2;
SSE = sum(resid.^2);
SSyy = sum((y-mean(y)).^2);
R2 = sqrt(1-SSE/SSyy)

end

% Plot results
loglog(x,y,'b+',X,Y,'r');
axis([.1 100000 10 10000]);
r = sprintf('%s at %s (%s)',P,T,m);
title(r);
xlabel('Shear Rate (1/s)');
ylabel('Viscosity (pa*s)');

% Display Parameters on plot
u = sprintf('tau= %1.2e',c);
v = sprintf('Vis(0)= %5.1f',Vo);
w = sprintf('n = %1.2f',n);
x = sprintf('r2 = %1.3f',R2);
y = sprintf('a = %4.3f',a);
text(1000,7000,s);
text(1000,4500,t);
if f == 1
    if f == 2
        text(1000,3000,u);
        text(1000,2000,v);
    else
        text(1000,3000,v);
    end
end
se
text(1000,3000,v);
id

f == 6
    text(1000,1000,w);
d

```

Viscosity Model Equations (vit.m function):

```
function err = fit(lambda)

global x y n f

if f == 1      % Bueche-Harding
err = sum((y-(lambda(2)./(1+(lambda(1).*x).^0.75))).^2);
end

if f == 2      % Eyring
err = sum((y-(lambda(2).*asinh(lambda(1).*x)./(lambda(1).*x))).^2);
end

if f == 3      % Carreau
err = sum((y-(lambda(2).*(1+(lambda(1).*x).^2).^(n-1)/2))).^2);
%err = sum((y-(lambda(2).*(1+(lambda(1).*x).^2).^(lambda(3)-1)/2))).^2); Not Used
end

if f == 4      % Cross
err = sum((y-(lambda(2)./(1+(lambda(1).*x)^(1-n)))).^2);
%err = sum((y-(lambda(2)./(1+(lambda(1).*x)^(1-lambda(3)))))).^2); Not Used
end

if f == 5      % Sutterby
err = sum((y-(lambda(2).*(asinh(lambda(1).*x)./(lambda(1).*x)^(1-n)))).^2);
%err = sum((y-(lambda(2).*(asinh(lambda(1).*x)./(lambda(1).*x)^(1- Not Used
lambda(3))))).^2);
end

if f == 6      % Vinogradov
err = sum((y-(lambda(2)./(1+lambda(4).*(lambda(1).*x)^(1-
n)/2)+(lambda(1).*x)^(1-n)))).^2);
%err = sum((y-(lambda(2)./(1+lambda(4).*(lambda(1).*x)^(1- Not Used
lambda(3))/2)+(lambda(1).*x)^(1-lambda(3))))).^2);
end
```

WORKS CITED

- 1 Rosen, S. L., *Fundamental Principles of Polymeric Materials*, Second Edition, John Wiley & Sons, Inc., New York (1993): 62-63.
- 2 Al Ghatta, H., S. Cobror and T. Severini, "New Technology for Solid-State Polymerization of Polymers: Polyethylene Terephthalate Solid State Polyaddition", *Polymers for Advanced Technologies*, 8 (1997): 161-168.
- 3 Moore, et al., "Process for Preparing High Molecular Weight Polyesters", U.S. Patent No. 4,446,303 (1984).
- 4 Thomas, et al., "Polycarbodiimide Modification of Polyesters for Extrusion Application" U.S. Patent No. 4,071,503 (1978).
- 5 Al Ghatta, et al., "Foamed Cellular Polyester Resins and Process for Their Preparation", U.S. Patent No. 5,422,381 (1995).
- 6 Xanthos, M., et al., "Effects of Resin Rheology on the Extrusion Foaming Characteristics of PET" *Proceedings from SPE ANTEC* (1998).
- 7 Xanthos, M., V. Tan and A. Ponnusamy, "Measurement of Melt Viscoelastic Properties of Polyethylenes and Their Blends - A Comparison of Experimental Techniques", *Polymer Engineering and Science*, 37, 6 (June 1997): 1102-1112.
- 8 Randall, C. S., "Predicting Extrusion Die Swell Using Flow Analysis", *Proceeding from SPE ANTEC* (1991): 4-7.
- 9 Pliskin, I., "Observations of Die Swell Behavior of Filled Elastomers Measured Automatically with a New "Die Swell Tester" ", *Rubber Chemistry and Technology*, 46 (1973): 1218.
- 10 Van Buskirk P. R., "Practical Interpretation of Laboratory Die Swell Behavior of PVC Extrudates - Through Correlating Circular with non-Circular Die Performance", *SPE Vinyl RETEC '89 Atlanta* (Oct. 1989): 105-133.
- 11 Maxwell, B., "The Melt Elasticity Index: A Quality Control Measure", *Plastics Engineering* (Sept. 1987): 41-44.
- 12 Villian, F., J. Coudane and M. Vert, "Thermal Degradation of Polyethylene Terephthalate: Study of Polymer Stabilization", *Polymer Degradation and Stability*, 49 (1995): 393-397.

- 13 Rosen, S. L., *Fundamental Principles of Polymeric Materials*, Second Edition, John Wiley & Sons, Inc., New York (1993): 271-272.
- 14 McCrum, N. G., C. P. Buckley and C. B. Bucknall, *Principles of Polymer Engineering*, Oxford University Press, New York (1994): 112-122.
- 15 Dealy, J. M., *Rheometers for Molten Plastics: A Practical Guide to Testing and Property Measurement*, Van Nostrand Reinhold Co., New York (1982): 50-53.
- 16 Bird, R. Byron, R. C. Armstrong and O. Hassager,, *Dynamics of Polymeric Liquids: Volume 1 Fluid Mechanics*, John Wiley & Sons, New York (1977): 192-193.
- 17 Rosen, S. L., *Fundamental Principles of Polymeric Materials*, Second Edition, John Wiley & Sons, Inc., New York (1993): 250-154.
- 18 Brydson, J. A., *Flow Properties of Polymer Melts*, Van Nostrand Reinhold Co., New York (1970): 47-50.
- 19 Abdel-Khalik, S. I., O. Hassager and R. B. Bird, "Prediction of Melt Elasticity from Viscosity Data", *Polymer Engineering and Science*, 14, 12 (Dec. 1974): 859-866.
- 20 Brydson, J. A., *Flow Properties of Polymer Melts*, Van Nostrand Reinhold Co., New York (1970): 65.
- 21 Liang, J. Z., "Research into Polymer Melt Die Swell during Extrusion", *Plastics, Rubber and Composites Processing and Application*, 15 (1991): 75-77.
- 22 Liang, J. Z., "A New Short Die Swell Equation for Polymer Extrusion", *Plastics, Rubber and Composites Processing and Application*, 23 (1995): 93-95.
- 23 Leblanc, J. L., "Factors Affecting the Extrudate Swell and Melt Fracture Phenomena of Rubber Compounds", *Rubber Chemistry and Technology*, 54 (1981): 905-929.
- 24 Gordon, G. V., M. T., *Shaw Computer Programs for Rheologists*, Hanser/Gardner Publications, Inc., New York (1994): 221-242.
- 25 Marsden, J. E., A. J. Tromba, *Vector Calculus*, Fourth Edition, W. H. Freeman and Co., New York (1996): 246-247.
- 26 Biran, A. and M. Breiner, *MATLAB for Engineers*, Addison-Wesley Publishing Co., New York (1996): 386-388.
- 27 Brydson, J. A., *Flow Properties of Polymer Melts*, Van Nostrand Reinhold Co., New York (1970): 63-69.

- 28 Rosen, S. L., *Fundamental Principles of Polymeric Materials*, Second Edition, John Wiley & Sons, Inc., New York (1993): 249-250.
- 29 Elbirli, B. and M. T. Shaw, "Time Constants from Shear Viscosity Data", *Journal of Rheology*, 22, 5, (1978): 561-570.